Aalto-yliopisto
Aalto-universitetet
Aalto University

Master's Programme in Biological and Chemical Engineering for a Sustainable Bioeconomy (BIOCEB)

Microencapsulation of Curcumin dye with ß-Cyclodextrin embedded in Ioncell® fibres by means of dry jet wet spinning

Hadiqa JAVAID

Master's Thesis
2022

Aalto-yliopisto
Aalto-universitetet
Aalto University

Author Hadiqa Javaid		
Title of thesis Microencapsulation of Curcumin dye with ß-Cyclodextrin embedded in Ioncell® fibres by means of dry jet wet spinning		
Programme Erasmus Mundus Joint Degree for Biological and Chemical Engineering for a Sustainable Bioeconomy (BIOCEB)		
Major Materials and Biopolymers		
Thesis supervisor Prof. Vuorinen Tapani & Prof. Andres Krumme		
Thesis advisor(s) Dr. Inge Schlapp-Hackl, Prof. Ali Tehrani		
Date 1.07.2022	**Number of pages** 52	**Language** English

Abstract

Development of regenerated cellulosic fibres (RCFs) opened up new ventures into the world of sustainable textiles. IONCELL® is a sustainable process which utilizes the IL, [DBNH][OAc] to dissolve cellulose. Through dry-jet wet spinning RCFs with great properties are generated which might be turned into functional textiles. Various spin solutions were prepared by mixing 1% curcumin and/or 2% ß-CDs with standard kraft bleached pulp dissolved in [DBNH][OAc]. Fibers were produced through the IONCELL® process and analysed in detail. All the properties were compared with IONCELL® standard fibers. The properties of all dopes were tested by rheology. The complex viscosity and dynamic moduli of the viscoelastic solutions were close to the standard IONCELL® dope. The presence of microcapsules of ß-CD with curcumin were confirmed by FTIR, XRD, DSC and TGA techniques. The mechanical properties of the generated fibres such as orientation was as high as 0.80 ± 0.12 with an average dry tenacity of 43.6 ± 5.4 cN/dtex. The colour stability of the spin-dyed fibres was compared with fibres dyed by post spinning through 30% ethanol solution. Washing fastness values for spin-dyed fibres was as high as 5 for both colour change and staining. The fibers showed a crystallite size of 41.4 ± 1.0, 35.5 ± 0.1 and 35.8 ± 0.2 Å for ($1\bar{1}0$), (110) and (020) regions for the cellulose-II polymorph, respectively. CRI was as high as 79.1 ± 0.7% which is very close to standard IONCELL® fibre. The amount of fixed ß-CD onto the fibres was quantified. With a 2 % addition of ß-CD on pulp 0.1 ± 0.03% ß-CD was fixed onto the regenerated fibres.

Keywords Cyclodextrin, Ioncell, Dry jet-wet spinning, Curcumin, Spin dyeing

Kokkuvõte (eesti keeles)

Taastatud tsellulooskiudude (RCF) arendamine avas uusi võimalusi säästva tekstiili maailmas. IONCELL® on säästev protsess, mis kasutab tselluloosi lahustamiseks IL, [DBNH][OAc]. Kuiv- ja märgketruse abil tekivad suurepäraste omadustega RCF-id, mida võib muuta funktsionaalseteks tekstiilideks. Erinevad ketruslahused valmistati, segades 1% kurkumiini ja/või 2% ß-CD-d standardse kraftvalgustatud tselluloosi, mis on lahustatud [DBNH][OAc]-is. Kiudusid toodeti IONCELL® -protsessi abil ja neid analüüsiti üksikasjalikult. Kõiki omadusi võrreldi IONCELL® standardkiududega. Kõigi dopingute omadusi kontrolliti reoloogiliselt. Viskoelastiliste lahuste kompleksviskoossus ja dünaamilised moodulid olid lähedased IONCELL® standardvärvainetele. ß-CD ja kurkumiini mikrokapslite olemasolu kinnitati FTIR-, XRD-, DSC- ja TGA-meetoditega. Loodud kiudude mehaanilised omadused, nagu orientatsioon, olid 0,80 ± 0,12 ja keskmine kuivsulavus 43,6 ± 5,4 cN/tex. Spinnvärvitud kiudude värvi stabiilsust võrreldi kiududega, mis olid värvitud 30%-lise etanoolilahuse abil pärast ketramist. Spinnvärvitud kiudude pesukindlus oli nii värvimuutuse kui ka värvimuutuse puhul 5. Kiudude kristallisuurus oli vastavalt 41,4 ± 1,0, 35,5 ± 0,1 ja 35,8 ± 0,2 Å ($1\bar{1}0$), (110) ja (020) tselluloos-II po-lümorfi piirkondades. CRI oli 79,1 ± 0,7%, mis on väga lähedal standardse IONCELL® kiu väärtusele. Kiududele kinnistunud ß-CD kogus määrati kvantifitseeritult. 2 % ß-CD lisamisel tselluloosile fikseeriti regenereeritud kiududele 0,1 ± 0,03 % ß-CD.

Contents

Preface

I want to thank Professor Tapani Vuorinen for including me in his research and for this project and my advisor Dr. Inge Schlapp-Hackl who has been extremely helpful and patient with me during my thesis journey. I also thank my advisor Prof. Ali Tehrani for his help in the dyeing portion of the work and Prof. Michael Hummel, for his guidance. I thank all those people in the labs who have helped me figure out my work in any way. My friends have been very helpful and a constant support in this time that I have spent in Finland and by the end of this thesis, I have found myself closer to them. I am lucky to have them as my friends in a place where you are all alone and the only thing close to family is your friends.

Moving here to Europe two years ago when I started this master's program and when I left behind everything will always be a life-changing decision. Even though I was happy to leave and explore new things, I will always remember that last hug that I had with my father. I wish you were here to see that I have graduated now but unfortunately you were gone too soon. When I left that night hugging you for the last night, I had never thought it will be my last hug and I will never see you again. But you were gone just after that. I hope that I am making you proud by doing what I am doing out here in another part of the world.

I want to thank my father (Javaid Akhtar Lak) who made me who I am today, you will always be in my heart and soul, Abu. I will not forget the things my mother and my sisters sacrificed for me to be here and to experience all this. I hope I make you all proud!

Otaniemi, 26 June 2022
Hadiqa Javaid

1 Introduction

The textile industry is one of the biggest contributors to environmental pollution with the use of toxic chemicals, increasing microplastic pollution and green-house gas emissions (Royer et al., 2021). Development of regenerated cellulosic fibres (RCFs) opened up new ventures into the world of sustainable textiles. Currently, Viscose and Lyocell processes are the two most used processes for the production of RCFs. The Viscose process releases toxic chemicals into the environment which are hard to recycle and the NMMO-based Lyocell technology even though closed-loop, has the problem that the solvent is unstable and an addition of stabilizers is needed (Kaniz, 2022). These problems promoted the development of the IONCELL® process which uses [DBNH][OAc] or other ionic liquids to dissolve cellulose and generate fibres using just a water bath. The IL can be recycled, which makes it a close loop process (Elsayed et al., 2020).

To understand the IONCELL® process, we first need to understand the structure of cellulose. Cellulose is the most abundant polysaccharide on earth made of anhydrous β-D-glucopyranose units bonded by (1-4)-glycosidic bonds. Cellulose has both a reducing end (C_1-OH) and a non-reducing end (C_4-OH). The OH groups on C_2, C_3, C_6 create H-bonds within the same chain (intramolecular) and also with adjacent chains (intermolecular). These H-bonds create the possibility of a supramolecular structure. Cellulose can be interconverted into six polymorphs but cellulose I and II are the most studied (Maurer et al., 2013). Cellulose-II is also called regenerated cellulose as it can be converted from cellulose I through regeneration or mercerization. Cellulose II has antiparallel arrangement of chains with more H-bonds and shorter distances between them, which makes it more thermodynamically stable (Figure 1) (Rowell, 2005).

Functional textiles are textiles with specific properties like increased hydrophobicity, antimicrobial/antifungal textiles, flame retardent, color sensing textiles, UV protection, fragranced and dyed textiles, etc. (Haji, 2020). These properties are induced by modifying the cellulose, or through microencapsulation. Microencapsulation usually involves the inclusion of a guest molecule (acting as a core) within a host molecule (shell) (Figure 2). Microencapsulation can be performed with chemicals like starch, composites and cyclodextrins, etc. Cyclodextrins (CDs) are cyclic oligosaccharides produced as result of enzymatic degradation of starch. The three most-abundant types are α (6 glucose units), ß (7 glucose units), and γ-cyclodextrins (8 glucose units). The glucose units are linked together by α-1,4-glycosidic bonds. ß-CD is the most studied CD. It is a hollow bowl-shaped molecule with its cavity being hydrophobic and outer layer being hydrophilic (Figure 2A). The OH groups present in the structure can allow unlimited modifications made to the molecule. But on its own, ß-CD is able to trap many molecules within its

central cavity. It is able to make inclusion complexes in 1:1, 1:2, 2:1 and 2:2 (Figure 2B) (Morin-Crini et al., 2021).

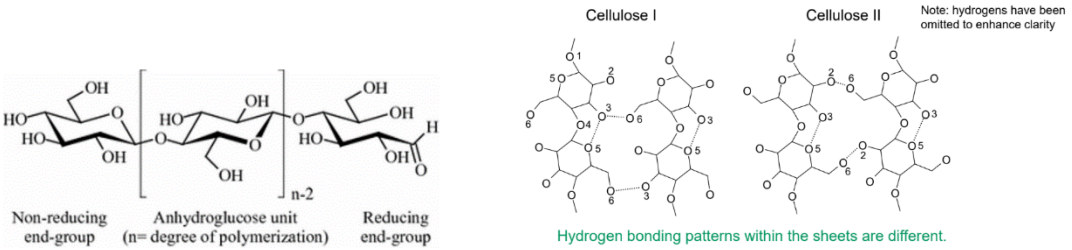

(A) **(B)**

Figure 1: **(A)** Structure of cellulose (Heinze et al., 2018) and **(B)** H-bonding patterns in cellulose-I and cellulose-II polymorphs (Kontturi, 2021).

The textile dyeing industry is infamous in the use of toxic chemicals making it a potentially high carbon impact industry. The trends recently have shifted towards the use of natural plant-based dyes without the use of extra chemicals. However, natural dyes are a challenge in their own because they're unstable and have low potential for chemical reactions. Curcumin (diferuloylmethane; 1,7-bis(4-hydroxy-3-methoxy-phenyl)hepta-1,6-diene-3,5-dione) also is an example of such a dye. It is a component of Turmeric plant: *Curcuma longa* which has multiple therapeutic benefits (Patel, 2011). The structure of curcumin is shown in Figure 3. Curcumin is a bis-α,β-unsaturated β-diketone and this form exists in equilibrium with its enol tautomer. The keto form predominates in acidic/neutral aqueous solutions and in cell membranes. On the contrary, the enol form of the heptadienedione chain preponderates in alkaline medium. Moreover, it is prone to degradation by UV light and is insoluble in water, but soluble in organic solvents like ethanol, acetone, DMSO, etc. These limitations make it a hard unstable dye to be used in textiles (Gupta et al., 2012).

The objectives of this research work involve the use of the IONCELL® technology to prepare curcumin added functionalized fibres through dry jet-wet spinning. This research work explores the potential of ß-CD for incorporating curcumin and dyeing the fibre during spinning. The work also compares traditional dyeing after the spinning with spin dyeing as a sustainable alternative by using natural dyes.

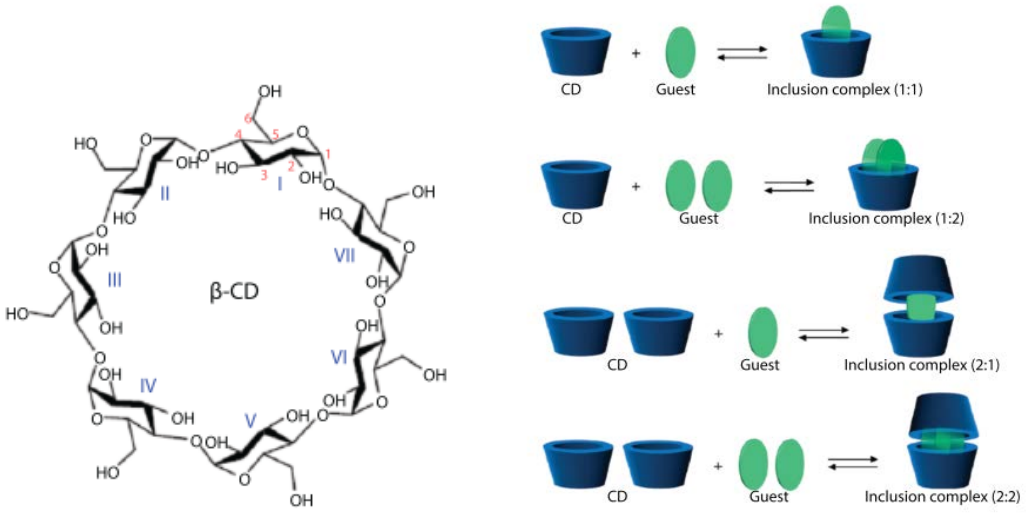

(A) **(B)**

Figure 2: **(A)** Structure of ß-CD and **(B)** possible types of inclusion complexes with ß-CD (Haji, 2020).

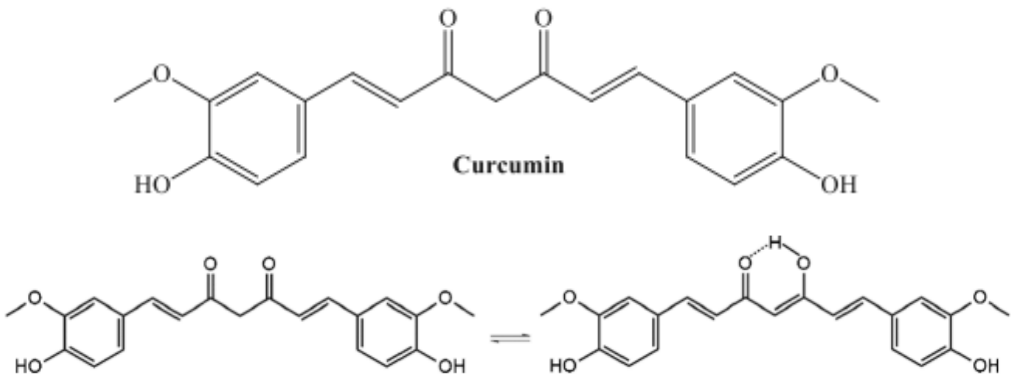

Figure 3: Chemical structure of curcumin (top) and its keto-enol tautomerism (bottom) (Stanić, 2017).

2 Literature Review

In this section, a review of some previous works related to the developments and areas of applications of Cyclodextrins (particularly ß-CD) with regards to the microencapsulation techniques along with the scope of application of curcumin dye (Figure 2A, 3-top) in the textile sector will be discussed. Some of the discussions will focus on the IONCELL® process and its developments in different applications particularly in fiber production.

Hilaire de Chardonnet was a French engineer working with Louise Pasteur on the renewal of the French silkworm industry damaged by the epidemic in the late 1870s. He discovered nitrocellulose when he failed to clean up a spill in the darkroom. This led to the development of the first artificial silk fibre of the world, which he called "Chardonnet silk" and introduced it in Paris in 1889. It was extremely flammable as it was nitrocellulose and wasn't much of an interest to the textile industry (Lewin, 2006).

The carbohydrate cellulose was discovered even before the first artificial silk fibre. It was discovered in 1838 by another French chemist, Anselme Payen, who determined its chemical formula and isolated it from plant matter. It was then first used to produce a thermoplastic polymer, celluloid in 1870 and led to the production of artificial silk (rayon) in 1890s. In 1912, cellophane was invented. In 1839, cellulose acetate was used to produce films and its first commercial use in the textile industry as a fiber was established by the Celanese company in 1924 (Malcolm et al., 2007). Cellulose is used in two ways: regenerated or pure cellulose such as used in the cuprammonium process and in its modified form such as cellulose acetate. The cuprammonium process was first discovered in 1927 by Schweizer (Schweizer, 1857) who found that cellulosic fibres e.g., from hemp and cotton are readily dissolved in a cuprammonium hydroxide solution. This was the process utilized for making Rayon fibres. However, a disadvantage of this process was the toxicity of copper sulphate which requires complete recovery from the process. This limits its large-scale production (Pfennig, 1995).

Viscose (Rayon) is the most famous man-made fibre and the technology for it has been evolved for 100 years. It is produced from cellulose obtained from wood or related agricultural products. In this process, the pulp is treated with aqueous NaOH (17-18%). This causes the fibres to swell and converts cellulose to sodium cellulosate. In the next steps, the swollen mass is pressed and shredded. This mass is alkali cellulose which is aged to reach the desired degree of polymerization (DP) of cellulose by oxidation and after that treated with CS_2 to form cellulose xanthate. This cellulose xanthate is dissolved in diluted NaOH to get a viscous orange solution which is called viscose. This final solution is filtered and ripened until ready for spinning. Next fibers are produced by wet spinning and cellulose is regenerated and recovered using a diluted H_2SO_4 bath. There are multiple drawbacks of this

technique like poor resiliency of the fibres and high pollution loads (Sayyed et al., 2019).

For making cellulose acetate fibres, pure cellulose fibre is first treated with a mixture of acetic anhydride, acetic acid and concentrated sulfuric acid (catalyst). The mixture is ripened, and the cellulose acetate flakes are precipitated and finally dissolved in acetone. Even though, this process makes fibres or textiles with a good draping ability, easy to handle and comfortable; it has poor physical strength and creates a lot of acetone pollution with hazardous by-products (McKeen, 2012).

The Lyocell process is the most promising technology compared to the above-mentioned processes. It involves the non-derivative route to cellulose dissolution in an organic and aprotic solvent: N-methyl morpholine N-oxide (NMMO). This solvent dissolves cellulose directly. It is a short process (3-4 hours) and has a much better efficiency. Another advantage of this process is that no derivatization of cellulose is required, no aging of cellulose is needed, consequently the DP of cellulose can be preserved to the maximum and lastly very few chemicals are needed for this process. The NMMO solvent used can be recovered (98.5 – 99%) and it is non-toxic, biodegradable and environmentally harmless. The fibres produced from Lyocell process are called Tencel® (Jiang et al., 2020).

The NMMO-based Lyocell process is the only alternative to viscose fibres. It should be mentioned that the NMMO-water and cellulose system goes through many side reactions. These side by-products affect the properties of the fibres. For the prevention of these side by-products, stabilizers are needed to prevent dangerous runaway reactions. But the use of a stabilizer still doesn't guarantee a risk-free process (Rosenau et al., 2001). Even though, there have been some other cellulose solvent systems, up to now Lyocell is the only commercialized technology. Nonetheless, it is still not very readily employed as much as the Viscose process. This led to further research in using different ILs for dissolving cellulose and spinning them into fibres using dry-jet wet spinning processes.

Ionic liquids (ILs) have recently emerged as benign solvents, which are able to dissolve cellulose well. Swatloski et al., (2002) reported the dissolution of cellulose without derivatization in ILs such as 1-butyl-3-methylimidazolium chloride ([C_4mim]Cl). This study opened a whole new branch for cellulose dissolution and cellulose solvent systems. Since then, there has been a plethora of reports on the characteristics of hundreds of ILs used to dissolve cellulose and discussions of their advantages and disadvantages. A summary of these ILs are given in a review by Wang et al., (2012). Although, most of them can dissolve cellulose, only a few of them have been able to be used to produce cellulosic fibres. These first-generation ILs have an imidazolium-based cation and chloride anion. But the corrosive character of their halides towards metallic equipment and their high melting points have led to the development of new ILs with acetate and dialkylphosphate anions.

Hummel et al., (2014) presented a novel IL 1,5-diazabicyclo[4.3.0]non-5-enium acetate ([DBNH][OAc]) for cellulose fibre spinning through dry-jet wet spinning. This process is called IONCELL® process. This IL is an amidine based organic solvent and not imidazolium based. The possibility was reported to dissolve high concentrations of cellulose (13%) at moderate temperatures (75-80^{o}C). Even at these high pulp concentrations, fibres were spun at temperatures lower compared to the Lyocell type process utilizing NMMO. The spinning was performed in a customized laboratory piston spinning unit used for dry jet wet spinning with water only as coagulation medium. The maximum DR achieved was 18 and fibres had excellent mechanical properties. The fibres were highly oriented (0.6 – 0.8) and showed a homogenous crystallinity (CRI 28 – 36%). All fibres displayed an elongation up to 22% and a tenacity up to 50cN/tex. The fibres were also spun into yarn and knitted into a fabric.

Next the stability of spinning and influence of other parameters like extrusion velocity, DR, spinneret dimensions etc. were analysed in detail. Hauru et al., (2014) aimed on the production of stronger cellulosic fibres with [DBNH][OAc], with a dope of 13% cellulose concentration, spun at extrusion velocities ranging from 0.02 – 0.04 ml/min, DR from 7.5 – 12.5. The produced fibres showed high tenacities (~552 MPa) and elastic moduli (~3.1 GPa). Moreover, it was found that the tenacity, resilience, birefringence and modulus are not dependent on extrusion velocity. The fibres achieved showed reduced properties due to some machine failures but were comparable to NMMO-based Lyocell fibers.

In 2015, the group was able to report the production of cellulosic fibres from [DBNH][OAc] at an official level and called it IONCELL-F® fibre. In this study, the effect of different cellulosic concentrations (10, 13, 15 and 17%) and DRs (0.9 – 14.1) on fibre properties was analysed. High tenacity fibres were produced from these cellulosic concentrations. It was found that in case the cellulose concentration was increased from 13 – 15%, it resulted in strong orientation of the cellulose chains. This in turn provided fibres with tenacities exceeding 50 cN/tex (both wet and dry) and even at moderate DRs the initial modulus was over 30GPa. This study illustrated also the high-performance of IONCELL-F® fibers in textiles. A knitted dress and scarf in collaboration with the Swedish School of Textiles in Borås and the famous Finnish textile and clothing design company Marimekko® was manufactured (Sixta et al., 2015).

After this, several studies were done and the influence of various process parameters on the properties of fibres were analysed. For instance, Hauru et al., (2016) compared the fibre properties prepared by [DBNH][OAc], 1-Ethyl-3-methylimidazolium acetate ([Emim][OAc]) and 1,1,3,3-tetramethylguanidinium acetate ([TMGH][OAc]). The results showed that dopes prepared with [TMGH][OAc] and Emim[OAc] are poorly spinnable while dopes in [DBNH][OAc] can be spun at DRs as high as 12.5. These poorly spinnable

dopes were solidified gels. Fibres from [TMGH][OAc] at DR 2 were poor in strength (tenacity of 10.9 cN/tex) and showed a very low resilience (0.54 MJ/m^{-3}). These fibres had no measurable birefringence. On the other hand, fibers from [Emim][OAc] were low in orientation but high in elongation. Spinning was only possible at lower DRs. In contrast, the fibres prepared from [DBNH][OAc] formed highly oriented fibres even at DRs as low as 2 and improved properties. A poor spinning is caused by dopes which are gelatinous having a pre-formed gel network before regeneration and by dopes which become weaker in the presence of water.

Stepan et al., (2016) worked on IONCELL-P(ulp), where paper pulp was converted into a dissolving pulp with IL and water mixture. In this work, IONCELL-P(ulp) and IONCELL-F(ibre) processes were combined into one process, using the same IL ([DBNH][OAc]). Birch pulp in the form of paper sheets was ground using a mill and mixed in the IL (15%)-water mixture and agitated in water bath at a temperature of 60°C and filtered. Next the cellulose fraction was air-dried mixed with [DBNH][OAc] to make a dope. The dope was spun according to temperatures specified by rheological properties (in the range of 65 – 73°C). By the take-up velocity different DRs were tested. This study was also an attempt to realise a closed-loop business study where a single IL can be used for both processes. The IL had a moderate extraction ability on the pulp. This extraction led to a total residual xylan content of 7.5% which is over the targeted <5%. To improve this number, enzymatic pretreatment was applied to the pulp. Pulpzyme xylanase enzyme cocktail was used which led to a 5.2% residual xylan content. Another experiment was performed where the concentration of the pulp was lowered to 2% instead of using the typical 5%, which decreased the xylan content to 6.5%. The viscosity of the pulp before spinning was adjusted using an acidic treatment. This further decreased the xylan content to 5.8%. After combining all these pretreatments, a final residual content of 4.2% was achieved. The final fibres after spinning had a residual xylan percentage of 3.5%, a tenacity of 50.7 cN/tex and 23.6 GPa of young's modulus. These properties of the IONCELL-F fibers spun from IONCELL-P were comparable to the strength of fibres spun from commercial pre-hydrolyzed kraft pulps, lyocell and viscose fibres.

Hummel et al., (2018) tested the suitability of various starting materials like Eucalyptus pre-hydrolyzed kraft pulp (PHK), Birch PHK pulp, Birch ECF kraft pulp, cotton waste from hospital bed sheets, A4 copy paper sheets, cutting residues from Finnish fluting board mil for the fibre production by the IONCELL® technology using [DBNH][OAc] as a solvent. These materials contained not only cellulose but hemicelluloses and lignin as well. In case of paper and cardboard having 50% Organo Solv (OS) lignin, the concentration of solute had to be varied in a way to provide the required viscoelastic dope properties. The biopolymers once separated and mixed, showed no apparent interaction and hence no significant change in the elasticity of the polymers. In pulps where these polymers were not separated beforehand, a

considerable higher even gel-like consistency which makes the dope non-spinnable was noticed. A DR >10 was achieved for all dope samples. A higher cellulose content, led to higher tenacities of the fibres. Fibres spun from recycled cotton from hospital bedsheets consisted only of cellulose. Their tenacities reached around 60 cN/tex as opposed to fibres with 50% OS lignin which had the lowest tenacities (<25 cN/tex). A similar trend was observed for Young's moduli. The elongation decreased rapidly for all lignocellulosic solutes (8% for a DR over 4). This study concluded that even though cellulose acts as the major factor to govern the mechanical properties of a fibre, the non-cellulosic components affect the fibres to some extent as well. They act as a plasticizer and enhance the elongation at break properties of the fibres. But this effect was only pronounced in fibres with lignin content of >30%. Also, a correlation was found between cellulose content and high strength. Low molecular weight polymers (hemicelluloses and lignin) when spun are getting lost in the coagulation bath, which makes it difficult for the IL to be recycled.

In an another study, [DBNH][OAc] was compared with another guanidine-based IL: 7-methyl-1,5,7-triazabicyclo[4.4.0]dec-5- enium acetate ([mTBDH][OAc]). This study focused on the drawbacks and challenges coming up in the recovery of ILs. Dopes with both ILs were prepared and spun in compliance with the rheological properties. Certain modifications were made in the composition of [mTBDH][OAc] to adjust the acid/base values. However, it was found that any alterations affect the dissolution negatively and the solution kneading time for altered dopes was increased. Moreover, [mTBDH][OAc] also showed a higher resilience towards the presence of water. In the presence of 1% of water, the cellulose dissolution was >90%. As the water content was increased, the tolerance of the IL was decreased but compared to [DBNH][OAc] it was better even at a water content of 10%, with an acid/base ratio of 1.2. No other super-based IL at that time was reported which could dissolve 13% cellulose even at high rates of alterations. In all acid/base alterations of the [mTBDH][OAc], no changes in the viscoelastic properties such as zero-shear viscosities (η_o), angular frequency at the cross-over point (ω_{COP}), and dynamic moduli ($G' = G''$) were found. The average η_o value was 28,746 Pa.s, ω_{COP} of 0.88 s^{-1} and $G' = G''$ of 3874 Pa (at 85^{o}C). A high DR between 14 – 15 was achieved with no interruptions during spinning. As a comparison, the dissolution capacity of [DBNH][OAc] was already exhausted at an acid/base ratio of 1:1 (Elsayed, et al., 2020).

Guizani et al., (2020) reported new results related to the effects of air gap conditioning (AGC) on fibre properties during the spinning operation. This work also employed a new developed single filament spinning unit. Moreover, an air humidifier was used to project the air flow at a specific temperature. When the temperature was increased to 50^{o}C while the relative humidity (RH) was kept at 90%, the elongation of the fibres increased to 15.2% as compared to 12% without AGC. In another set of experiments, the extrusion

velocity (v_{ext}) was increased to 3.8 m/min resulting in a decreased elongation of 12.2%. In the optimization experiments, the v_{ext} and admissible air flow (F_{air}) were kept constant at 1.9 m/min and 10 l/min and the effects of temperature of air (T_{air}) and RH were investigated. The highest elongation (16%) was achieved when T_{air} was 30°C and RH was 70% compared to 12% elongation without AGC. With AGC, a 35 – 40 cN/tex tenacity was achieved. Moreover, with AGC the titre of the fibres was around 8 – 18% as compared to 25 – 30% without AGC. Curiously, no significant changes in orientation were observed with or without AGC.

The next study by Elsayed, Hellsten, et al., (2020) focused on the recyclability and spinnability of [mTBDH][OAc] through five cycles compared to [DBNH][OAc]. During the five cycles, the mass of the recovered [mTBDH][OAc] changed from 1.7kg (original) to 0.25kg. In the recovered solvent, 94.5 – 96.8 wt.% of total solvent was [mTBDH][OAc]. The residual water content of the recovered liquid was 2.6 – 3.1 wt.%, which is essential for the proper cellulose dissolution and maintenance of viscoelastic properties of the dope. In contrast, the recovery of [DBNH][OAc] after just one cycle gave 3.3 wt.% water, and 86.4 wt.% of IL. The neutral species in the ILs are the most vulnerable for vaporization. More neutral compounds in case of [DBNH][OAc] were removed compared to [mTBDH][OAc] during recovery. As far as the cellulose dissolution is concerned, it was possible to produce dopes in all 5 cycles using recovered [mTBDH][OAc]. On the contrary, dissolution of cellulose was halted just after a single recovered cycle of [DBNH][OAc]. Fibres spun from cycles 1.2 and 3 of [mTBDH][OAc] showed decent tenacities like fresh [DBNH][OAc] fibres. However, fibres prepared from cycles 4 and 5 recovered IL, showed tenacities and elongation values reduced to 38 cN/tex and 13.7%, respectively.

Further research in the optimization of the IONCELL® process, led to the development of a novel vertically arranged spinning bath for simulating a closed loop process. Dopes were prepared with the well-established IL [DBNH][OAc] and the properties of the fibres were measured after spinning by using the new bath. Besides various spinneret dimensions were tested. By the use of diverse L/D (Length to diameter ratio) DR<10 was always possible to reach. As the spinneret aspect ratio was increased, spinnability improved and DR 12 was reached. Tenacity of the fibres increased with higher DRs. At higher aspect ratio of the spinneret, the tenacity and elongation was higher. With 30% of IL in the spin bath DR12 was successful spun. With 45% of the IL in the bath DR8 was only reached. As this amount of IL concentration was increased to 60%, the maximum possible DR was 3. The fibre properties with this new spinning unit were good. The titre of the fibres was unaffected by the IL concentration but affected by the DR. The tenacity of the fibres increased until DR 8 and after that levelled off unaffected by the IL concentration. Fibre elongation was unaffected between 0 – 30 wt.% IL bath

concentration, but beyond 45 wt.% it decreased. The average crystallite size was 32 Å for all samples (Guizani et al., 2021).

Moriam et al., (2021) attempted to further enhance the strength and toughness of the IONCELL-F fibres. The factors considered were purity of the pulp, L/D (length to diameter) ratio of the spinneret and the concentration of cellulose in the dope solution. High purity pine (HPG) pulp was further purified and dissolved in melted [DBNH][OAc]. A higher DP of the cellulose was found in this pulp (1150) which leads to better orientation and stronger fibres. In the 13% concentration of HPG, an increased zero-shear viscosity was found. This provided better entanglements and hence better zero-shear viscosities. Increasing the HPG content from 13 to 15%, increased the zero-shear viscosity and moduli even further. With the help of simulations, it was found that the longer capillary length (L/D 2.0) helps to better align the fibres along their molecular axis. HPG fibres showed a higher toughness and tensile strength. Elongation was also increased for HPG fibres. At higher DRs (10 and 12), the toughness of the HPG fibres (13 and 15 wt.%) were around 70 – 80 MPa in the conditioned state. The same affect was observed in crystallite size, orientation and morphology of the fibres.

Even though the work on the IONCELL® process and its optimization is still on-going, various studies have been carried out further on the effect of the spinneret geometries and its impact on the strength of the fibres. Other important aspects under research currently are the incorporation of dyes via spin dying (Benjamin et al., 2016) and incorporation of various additives to improve diverse properties of the fibres like UV protection, hydrophobization and microencapsulation (Bojana & Marica, 2019). However, as far as the recent developments in the commercialization of the IONCELL® process are concerned, it has already reached pilot scale.

In analogy to all of these investigations this MSc thesis focuses on the production of fibres by means of the IONCELL® technique in combination with β-CD and curcumin. The fiber properties are analysed and compared to the results achieved by standard pulp.

In the following section the works related to the current developments in the use of CDs as microencapsulation molecules in different applications will be discussed. Besides, this research is the first attempt to incorporate the natural dye curcumin through the addition of ß-CD to the IONCELL® fibers by the lyocell type single and multi-filament dry jet-wet spinning techniques.

Cyclodextrins (CDs) were first discovered in 1891 when a French pharmacist and chemist, Antoine Villiers, was doing experiments on the reduction and degradation of carbohydrates under the action of ferments. He observed that unwanted crystals with specific properties were formed by enzymatic action on carbohydrates which were later called cyclodextrins. The first formation of CDs was observed in digests of *Bacillus amylobacter* i.e. *Clostridium butyricum* on potato starch under specific conditions. These crystals when purified had unique optical rotation and they were difficult to further

hydrolyse. Dextrins which have a high optical activity are stained red by Iodine and the intensity decreased with optical activity. Villiers continued to work on CDs and by manipulating certain experimental conditions, he was able to isolate the first two crystalline dextrins: α and ß-CD. He further found out that these two crystal isomers were insoluble in water, non-fermentable, acid-resistant, and soluble in alcohol. These crystals could also be transformed into ethers by using acid chlorides. This led Villiers to believe that the properties of these molecules were different from the polysaccharides and saccharides known at that time and hence he called them "*cellulosines*" because they were like cellulose (related difficulty of acid hydrolysis in both) (Viellers, 1891).

Franz Schardinger is considered as the "Founding Father" of CDs. At the beginning of the last century, in 1903, he observed that a highly-heat resistant bacteria dissolves starch to form crystalline by-products which were just like the crystalline products reported by Villiers. In 1904, he isolated a microorganism, which produced acetone and ethyl alcohol by fermentation of starch. It was named *Rottebacillus I* (later as *Bacillus macerans*) (Schradinger, 1905). Schradinger continued his research on the chemistry of CDs until 1911. In 1911, he called the discovered products "*crystallized dextrin- α*" and "*crystallized-dextrin- ß*". Finally at the end of 1940s, Cramer was the first one to propose a cyclo- nomenclature for these products. They were called as, (6-ose)-cyclodextrin for α-CDs, (7-ose)-cyclodextrin for ß-CDs and (8-ose)-cyclodextrin for γ-CD, respectively (Morin-Crini et al., 2021).

The first industrial CD related patent was published in 1953 by Freudenberg, Cramer and Plieninger. This patent focused on important applications of drug formulations and what affects could be achieved by complexation of the drugs with CDs. These effects include improving solubility of poorly soluble drugs, protection of highly volatile substances, protection of easily oxidized substances, etc. However, this patent had not found any industrial application (Cramer et al., 1951). In late 70s and 80s, the first industrial scale applications in pharmaceuticals appeared.

The first product containing CDs was marketed in Japan in 1976. This product was "prostaglandin E2/ β-CD" (Prostarmon E™ sublingual tablets) (Uekama & Hirayama, 1978). E2 prostaglandin has a potent oxytocin-like effect which was a subject of interest for inducing labor in child birth. But since oxytocin was highly unstable, it was complicated to develop a formulation. Hence, encapsulating it with α or ß-CDs in aqueous solution was attempted. It was found that the solubility of the hormone was better in ß-CD. Moreover, as the concentration of CD was increased from $(5 - 15) \times 10^3$ M, the concentration of the hormone increased the same way and was increasing linearly. After this, a dramatic development occurred for pairing different molecules with CDs.

The first food applications appeared when Japan in 1976 authorized the use of CDs as food additives. There were many marketed flavors available on

the market such as powdered flavors of spices, citrus fruits, apples, horseradish wasabi, mustard, peppermint etc. Some of the other marketed products included a chocolate (Choco Bar™), powdered green tea (Stick Lemon™) and chewing gum (Flavono™), etc. In 2000s, CDs were added to the safe list of food additives of the US Food and Drug Administration (FDA). These days, food and pharmaceutical industries are the industries which consume the highest amount of CDs. In 1981, CDs were first employed in analytical chemistry for the use in purification and chromatography methods. In the mid-1980s, CDs were introduced in cosmetics in products like Epicutin®, Vivace®, Klorane®, Novoflex® Revlon, Eucerin® Vital Active Beiersdorf, etc. Their use in textiles started in 1980s as well, for making functional textiles (Morin-Crini et al., 2021).

Minns & Khan, (2002) performed some studies on the formation of host-guest complexes of α-CD in combination with iodine and potassium iodide (KI). They prepared a solution of KI and iodine which resulted in the formation of triiodide ions (I_3^-), in excess of KI. In each ml of I_3^- solution, varied amounts of α-CD solutions and water were added at 15 and 25°C and the absorbance of these solutions was measured. It was found that up to a 15 x 10^5 M concentration of α-CD, the absorbance increases up to 0.8 at 360 nm. After this point, no increase in absorbance was reported at higher α-CD concentrations. This point was reached with a ratio of 2:1 of α-CD and I_3^- . Moreover, they studied the possible geometries of two possible types of inclusion complexes formed with α-CD. One type was the α-CDI_3^- with 1:1 complex composition and the other one was α-$CD_2I_3^-$ with 2:1 geometry having two molecules of α-CD trapping one molecule of I_3^- ion. In the 1:1 geometry, I_3^- ion was found perpendicular to the α-CD molecule plane. While in the 2:1 geometry, the I_3^- molecule was shifted from 90° to 30°. Besides, in the 1:1 complex, the I_3^- molecule is only bonded to one α-CD molecule and is exposed to solvent and might go through cleavage. On the other hand, in the 2:1 geometry of the complex, the I_3^- is bonded to two molecules of α-CD and is sandwiched between them. This sandwich protects the ion and is strongly bonded and less exposed to the solvent.

Li et al., (2017) performed a pulmonary delivery of tee-tree oil in ß-CD for treatment of fungal and bacterial pneumonia. The inclusion complexes were prepared by grinding method with a solution of tea tree oil (TTO):ethanol (1:1 v/v) and mixed with ß-CD. A simulated lung deposition of the complexes in the form of capsules was also performed and tested on rat models as well. FTIR results confirmed the formation of inclusion complexes between ß-CD and TTO. In the first stage of deposition in the lungs, the deposition was high (30%) and started decreasing at later stages. A high effect against fungi (*Candida albicans*) and bacteria (*Aceintobacter baumannii*) in the infected lung was found. This effect was between 10 – 15 (x 10^7/ml) colony forming units (CFU) for the microorganisms which is much higher than individual effects

of penicillin. Moreover, in this system no biocompatibility issues were encountered.

In another work by Santos et al., (2017), Methyl-beta-cyclodextrin (Mβ-CD) which is a modified form of β-CD were complexed with β-Caryophyllene (BCP) through kneading, lyophilization and rotary evaporation. The stability constant (K_s) of Mβ-CD/BCP inclusion complexes was 128 M^{-1} as compared to the Ks value of 125 M^{-1} for BCP/ hydroxypropyl-beta-cyclodextrin (HPβ-CD). The presence of inclusion complexes with Mβ-CD were analyzed with ^{1}H-NMR and FTIR studies. The pharmacological potential of the complexes in the form of a 50 mg oral solution was tested with classic animal models. In mice with Carrageenan-induced Paw Edema and Peironitis, the Mβ-CD/BCP complexes showed a significant anti-inflammatory and antioxidant activity. Moreover, they also had a preventive antioxidant effect on ethanol induced gastric damage.

Celebioglu & Uyar (2019) prepared inclusion complexes of HPβ-CD and Ibuprofen for making a fast-dissolving oral drug delivery system through electrospinning. Ibuprofen was inclusion-complexed with HPβ-CD in highly concentrated aqueous solutions of HPβ-CD (200%, w/v) having two different molar ratios: 1:1 and 2:1 (HPβ-CD/ibuprofen). These solutions were then electrospun and the nanofibers were deposited on a foil sheet. Such a high concentration of HPβ-CD made it possible to perform successful electrospinning. The average fibre dimensions of the HPβ-CD/Ibuprofen (1:1) complexes and HPβ-CD/Ibuprofen (2:1) complexes were 180 and 210 nm, respectively. The viscosity of these solutions was within a range of ~1.2 – 1.5 Pa.s and conductivity was within the range of ~35 - 45 μS/cm. These parameters yielded thin nanofibers. The presence of Ibuprofen in the complex was also confirmed by FTIR. The phase solubility studies showed that the concentration of the Ibuprofen was stable with HPβ-CD, and the absorbance of both 1:1 and 2:1 complexes, displayed equal absorbance, indicating a slower homogeneous release. Moreover, the nanofibrous sheets dissolved in water in less than 5 seconds for both 1:1 and 2:1 complexes.

In a study by Chang and colleagues (2021), Linalool-chemotype *Cinnamomum osmophloeum* leaf essential oil and its stabilization with β-CD as microcapsules was researched. Microcapsules were prepared by coprecipitation. The stability of the inclusion complexes (ICs) was studied using an accelerated dry-heating ageing test. For optimization of the IC composition, various concentrations of Linalool - β-CD mixtures were prepared by using a ethanol/water/β-CD solution. The highest yield of linalool in ICs was 94.2% with 15:85 (w/w) β-CD which was close to the molar ratio of 1:1. For the ICs prepared with ethanol/water/β-CD, the highest obtained yield was 98.1% by the use of 1:5 of ethanol/water. With the leaf essential oil, the optimum yield of linalool-chemotype ICs with β-CD was 96.5%. The stability studies suggested that in non-extruded starch only 8% of the limonene extract was found whereas it was up to 92.2% in ICs with β-CD. During the dry-heating ageing

period, the weight loss in the leaf essential oil ICs was 6.73, 9.33, 12.14 and 13.40% after 1,2,4 and 8 days of testing, respectively. This confirmed a stable and slower release of the oil from the ICs.

Sharma & Satapathy, (2021) prepared ICs of Polylactic acid (PLA) and Polycarpolactone (PCL) (70:30 w/w) with varying amounts of β-CD (from 0 – 20 phr) by electrospinning onto mats. The efficiency of the ICs and the physicochemical performance was tested. With increasing β-CD concentration, the average fibre diameter increased and a decrease in the viscosities was found. The average diameter of the fibres ranged from 0.7 – 1.7 μm when the concentration of the electrospinning solution was raised from 14 – 20 wt.%. Moreover, as the β-CD content was increased from 5 – 20 phr, the electrical conductivity of the electrospinning solution was decreased to 0.1 μS/cm. Porosity of the mats was high (54%) for the highest β-CD concentration (20 phr). Also, the contact angle values decreased from 139 – 132^{o} by decreasing the β-CD concentration from 0 – 20 phr. Young's modulus, elongation at break and tensile strength decreased to around 40MPa, 40% and 0.5 – 1.0 MPa with increasing β-CD concentration. For the detection of the efficiency of the ICs, the IC mats were immersed in an ethanol/water solution of curcumin and the change in colour of the solution was measured as a sign of binding of the curcumin molecules by the β-CDs at the mats. The higher the concentration of β-CD in the mats, the lower the concentration of curcumin in the solution was. With 10 phr of β-CD, curcumin concentration was decreased to 0.75 (ratio of later curcumin concentration compared with original, as it's a ratio between two concentrations, it has no units) per week.

The next section will focus on the developments of β-CDs in connection with functional textiles. The first industrial applications of microencapsules were introduced by Cash Register Company in 1950s for encapsulating leuco dyes for making carbonless copy paper. Functional textiles are a category of textiles which show modified properties due to the presence of additives or innovative functionalities or coatings. Few examples of these are permanently colored textiles, flame-resistant textiles, color changing textiles, thermal control textiles, UV protected textiles, superhydrophobic textiles, sound-absorbing textiles, biosensors, insecticide textiles, insect repellent textiles, fragranced textiles, antimicrobial textiles, medical textiles, cosmetotextiles and multifuctional textiles, etc. One of the first microencapsulation application in textile design was the microencapsulation of pigments and dyes (natural/non-natural (Podgornik et al., 2021).

Cireli & Yurdakul in 2006 used 8 different dyes on 100% bleached and mercerized cotton woven fabric in combination with β-CD. The colour fastness of the fabrics was measured by dye exhaustion and washing of the fabric. Until a certain point, the uptake of the dye stuff was increased but after this point, there was no further dye uptake. 0.5 g/L of β-CD in the dyeing liquor made no significant difference in the dyeing efficiency. But as the concentration was increased to 4 g/L, a significant decrease in the dyeing efficiency was

observed. The most pronounced decrease was observed for Orange KCF (20%). A levelling agent called Levegal ED which maintains this rate of exhaustion with dyes and helps to resist the decrease in the dye uptake was utilized. However, this levelling agent was found to have different effect on different dyes. But almost the same exhaustion results were observed for the levelling agent as with β-CD. The washing liquor of dyed textile was also tested with 5 g/L of β-CD. Different results were obtained with different dyes. This change was even more pronounced when the washing liquor was made with salt water and β-CD. In each of these cases, Orange KCF dye was the most affected.

The quantification of CDs and their extent of making microcapsules are an important aspect in terms of quality of the products. The quantification of CDs on textiles is difficult and the simplest method is the gravimetric determination. Another option for textiles with monochlorotriazine substituted β-CD (MCTβ-CD), is the triazine test and elemental analysis by determining the N2 content. However, each of these methods have their drawbacks. In an attempt to provide a better quantification of microcapsules on textiles, Grechin et al., (2007) prepared ICs of amines and alcohols etc. with β-CD and determined the amount of β-CD fixed onto cotton materials by titration of the extracted amines in water. The results showed that approximately 50% β-CD were able to from a complex with amines. The complexation was affected by the chain size of amines and their adsorption onto the textile. It was found that an increased chain size, implies a decrease in adsorption and a reduction in complexation.

Another development was made by Bereck (2010). Their method provided a direct determination of the actual binding ability of the natural or modified CDs on textiles without the need of a calibration curve/procedure. They chose ferrocene to form 1:1 ICs with β-CD. They also utilized different cellulosic cross-linking agents and the amount of fixation was measured. The cross-linking agent HMM was able to maintain 50% of the ICs even after 20 washing cycles. These cross-linking agents contained formaldehyde whose release was measured to estimate the effects of the β-CD. It was found that β-CD helped in the slowed of the release of formaldehyde.

Dehabadi et al., (2014) came up with a simple spectrophotometric determination of the amount of the fixed β-CD onto cotton fabric and their accessibility yield using Phenolphthalein and Phenol red dyes. The mole of the dye fixed onto the fabric was calculated using calibration curves of the dyes and then the total weight fraction of the fixed β-CD and their accessibility yield was calculated. However, first the cotton fabrics were immersed in a basic pH (pH 11) solution of 0.1g of the dyestuff in ethanol and water. The fabric was then dried and extracted in pure ethanol followed by washing with alkaline water. The washing liquor's absorbance values were then measured. This is also the method utilized in this research to quantify the amount of β-CD used in the fibres. Their results suggested that as the MCTβ-CD amount fixed onto

the fabric increased, the absorbance of the alkaline solution increased significantly. The weight fraction of fixed MCTβ-CD was always higher for phenol red than phenolphthalein. At a concentration of 4.95 gravimetric % of MCTβ-CD, the weight fraction of fixed MCTβ-CD in phenol red and phenolphthalein was 3.48 and 3.02%, respectively. The accessibility yield of MCTβ-CD with phenol red and phenolphthalein was 70.3 and 61%, respectively.

Arias et al., (2018) prepared citronella oil and β-CD ICs and fixed them onto cotton and spun polyester fabric through pad drying process. They also prepared liposomes with internal wool lipids (IWL) and phosphatidylcholine (PC) and fixed them onto cotton and other fabrics. The percutaneous absorption was measured using a Franz diffusion cell and multiple other subjects were subjected to exposure through a bandage over the period of multiple days. The release of the oil depended on the kind of fabric used for ICs with β-CD. It was found that 100% of the drug was released much quicker onto cotton fabric than onto polyester. In polyester, 100% of the drug was released at around 600 minutes while in cotton it was completely released at around 400 minutes compared to 200 minutes without ICs.

In 2021, Xiao and colleagues, came up with double encapsulated microcapsules of lavender essential oil and indigo dye with epichlorohydrin β-CD and fixed them onto cotton fabrics. The loading amount of lavender oil was 10% and indigo was loaded up to 9.73%. The fabrics treated with this solution changed the colour from white to blue with a nice lavender fragrance. The adsorption capacity of the double microcapsules increased with time. Within the first 50 minutes, it was rapidly adsorbed and gradually reached an equilibrium point. After 9 hours, the amount adsorbed was 116.6 mg/g. By testing the staining conditions, 4-5 color fastness level was observed in the first round of rubbing and in accelerated laundering, this value reduced to 2. After friction, the amount of fixed double microcapsules was 81,4%.

The next section will focus on works related to the use of curcumin in textiles, dyeing methods and the use of β-CD with curcumin to create functional textiles for a variety of applications.

Curcumin was discovered for the first time around two centuries ago by Vogel and Pelletier who first reported the isolation of a “yellow coloring matter” from the rhizome of the plant *Curcuma longa* (turmeric) and called it curcumin. Later it was found that this is a mixture of turmeric oil and resin. Vogel in 1842 then created a method for the extraction of pure curcumin but he didn’t know about its formula. In the following decades, many chemists were interested in curcumin and provided multiple possible curcumin structures. But in 1910, Milobedzka and Lampe were the first ones to identify the chemical structure of curcumin as “diferuloylmethane or (1E,6E)-1,7-Bis(4-hydroxy-3-methoxyphenyl)hepta-1,6-diene-3,5-dione”. In 1913, their group also were successful in synthesizing the compound followed by Srinivasan, who separated and quantified its components by chromatography. Even though turmeric has been used for various therapeutic applications for

thousands of years, the first paper on the biological effects of curcumin was published in Nature in 1949 by Schraufstatter and Bernt. They reported that it has antibacterial properties, and it is a biologically active compound. Their report found it active against bacteria like, *Mycobacterium tuberculosis*, *Staphylococcus aureus*, *Salmonella paratyphi*, *Trichophyton gypseum*, etc. (Gupta et al., 2012).

Curcumin is also used as a yellow-orange food coloring (E100) having a hot bitter taste and is approved by Food and Agriculture Organization (FAO). The safe amount of consumption per person per day for curcumin is quite high (8g/day). Hence, it is used in many applications in food packaging, as food additive, food preservation, as pH sensor to indicate alkaline compounds formed during food spoilage, etc. Metal oxide nanoparticles, chitosan nanoparticles with curcumin have been tested for their antimicrobial activities. Other applications in health care products include hydrogels for wound healing, microcapsules and microemulsions in dermal therapy and cosmetics, etc. (Raduly et al., 2021). The dyeing of textiles with natural pigments/dyes like curcumin still poses scientific challenges as these natural dyes are unstable and their incorporation in textiles is difficult.

Tsatsaroni et al., (1998) studied the dyeing properties of two yellow natural pigments: Crocin and curcumin and the effects of enzymes and proteins on these dyes. They used commercial bleached cotton and wool fibres for dyeing and used α-amylase and trypsin to treat the fabrics at 25^{o}C. They determined the amount of dyes by extracting the dye from the fabric via pyridine-water mixture and measured the absorbance of the extracts. Finally, they also tested the washing fastness of the dyed fabrics. It was found that the exhaustion of curcumin without any enzyme was 30% and the level 3-4 was reached by the fastness colour test for the cotton fibres. With trypsin, the exhaustion percentage increased up to 94.5 % at 60^{o}C. However, the colour fastness values dropped to 2-3 in wool fibres. After extraction of the wool samples with pyridine-water two extracts were collected, which had different absorbances at 440 nm and the intensity was 35% higher than the pretreated samples. Quantification of the released dyes within the extracted sample wasn't possible because of large amounts of pigments and other constituents in the extracts.

Sachan & Kapoor (2007) extracted curcumin from various samples of turmeric rhizomes through spray drying, aqueous and solvent drying methods. Spray drying gave the purest yield of curcumin while the highest yield was given by solvent extraction. With 2% concentration of the dye, they dyed cotton, wool and silk. A variety of shades through dyeing were obtained. These include yellow, ivory, golden, bright yellow, buff, khaki, golden yellow, smoke brown, cream, pineapple, lemon, olive green etc. The highest yield of curcumin obtained was 6.6% in one of the turmeric samples. They utilized mordants like myrabalon extract, eucalyptus bark extract, aluminium sulphate, copper sulphate, ferrous sulphate, stannous chloride, lactic acid and acetic

acid. The fabrics were pre-treated with these before dyeing. The optimized conditions of dyeing were 50-60^{o}C, 2% concentration of curcumin for 30 minutes and 60 minutes for a darker color. 10% myrabalon, 5% other chemical mordants and 1% eucalyptus dye mordant was enough for pre-fixation and mordanting.

In another study by Ammayappan & Jeyakodi Moses (2009), the antimicrobial activity of cotton, wool and rabbit hair was studied using aloe vera, chitosan and curcumin. They treated the cotton fibres with peroxide and wool and rabbit hair with formic acid to improve the dye exhaustion. They found that the add-on of curcumin was much lower compared to aloe vera and chitosan but was better for all treated samples. Peroxide cotton accumulated 1.80% of the curcumin as compared to 1.31% in treated wool and 1.11% in treated rabbit hair. The antimicrobial effect of curcumin was the highest. At 10^{-3} dilution, 2 bacterial colonies were found in cotton, 4 in wool and 1 in rabbit hair. As for the anti-fungal effect, the effect of aloe vera was the same as curcumin.

Paramera et al., (2011) published a study in which they report the stability and release properties of curcumin encapsulated by yeast (Saccharomyces cervisiae), ß-CD and modified starch. The encapsulation yield (EY%) of dye with ß-CD ranged from 3.4 – 0.8% and was much lower compared to yeast (31 – 39%). This was also the case in encapsulation efficiency (EE%) where for yeast it was around 88% and for ß-CD it was 22 – 17%. In in-vitro studies conducted in simulated gastric fluid and pancreatic fluid, it was found that ß-CD released the highest amounts of curcumin in the first 10 minutes and after that the release was stable until 70 minutes. But with yeast and modified starch (MS), the release was fluctuating and these released lower amounts of curcumin. After 30 minutes in simulated gastric fluid, ß-CD released lower amounts of curcumin. The light stability studies showed, that yeast was found much better in retaining curcumin for 1 month as compared to ß-CD. After 1 month, ß-CD enclosed only 60% of the curcumin while yeast contained around 90%.

Reddy et al., (2013) studied the antimicrobial activity of cotton and wool fabrics dyed with curcumin. Even at low curcumin concentration of 0.01%, 77% of the bacteria *Staphylococcus aureus* was inhibited but *Eschrechia coli* inhibition required a larger concentration of curcumin (10 times more). A similar effect was found in wool fabrics. The color depth values (K/S) indicate the concentration of curcumin added onto the fabric. It was seen that for *S. aureus* the colonies increased at a K/S value of 2 and after that levelled off meaning that they were not growing anymore. For *E. coli* this effect was lesser and was not achieved until K/S value 6. After laundering and light exposure, the antimicrobial effect of the fabrics was tested for 30 washing cycles. The cotton fabric was durable enough to reduce the colonies up to 20% in 30 washing cycles for both bacteria, but the effect was more pronounced for *E. coli*. Curcumin had poor resistance to light. The fabrics faded only after

5 units of light exposure hence, the fabrics had a low light fastness. The faded fabrics still showed good antimicrobial activity and reduced the population of S. aureus from 76 – 87% after 5 light exposure units. For E. coli, its population reduced drastically from 73 – 25% after 5-light exposure units.

In a study conducted by Sun et al., (2013) electrospun Polyvinylacetate (PVA) loaded fibres with curcumin and ß-CD were prepared and their in-vitro drug release potential was tested. The average fibre diameter was higher for complexes with just PVA/curcumin. As the concentration of curcumin was increased from 5 – 20 wt.%, the average fibre diameter for PVA/curcumin complexes dropped from 350 – 250 nm. The drop in diameter was less in case of PVA/curcumin and ß-CD complexes. The drop was from 300 – 270 nm caused by an increase of the concentration from 20 – 50 wt.%. In the drug release profiling, the PVA/curcumin fibers (5% curcumin consistence) released almost 95% of the curcumin within the first 150 minutes. In case of 15 wt.% curcumin consistence, the release was reduced and after 350 minutes, only 80% of the curcumin was released. On the contrary, in PVA/curcumin and ß-CD complexes, the lowest concentration of curcumin showed the best results in dye release. It released only 60% of the drug at 350 minutes.

Hasan et al., (2014) dyed cotton and silk fabrics with pure naturally extracted curcumin dye using the mordants aluminum sulphate ($AlK(SO_4)_2.{}_{12}H_2O$), copper sulphate ($CuSO_4$) and tartaric acid ($C_4H_6O_6$). The results revealed that methanol was the best in extracting the most curcumin (5.25%) and then ethanol (5.15%). The color strength (K/S) and the pH sensitivity were tested. They found that silk had a much better K/S value (20) in fabrics of 10% of dye while in cotton this strength remains unchanged (5-8) at the concentration range of 2 – 10 wt.%. From pH 3- 7, silk had around 13 – 17 K/S values while in cotton these values were 5 – 8 K/S. As pH was increased to 9, the fabrics lost almost all color. Silk had significantly higher K/S values than cotton when changing the dye bath temperature from 60 – 100^{o}C, For silk, the highest K/S value (18) was reached at 75^{o}C while cotton showed no effect. Besides, the fabrics were not affected by the dyeing time. In silk, even though the strength was much higher, there was no time dependencey and the same was observed for cotton. The type of mordants also had no effect on the change in dyeing strength of both silk and cotton fabrics. But the use of mordants slightly increased the K/S value for silk (20) and for cotton it increased it to 9. For cotton, $CuSO_4$ was the best mordant and for silk, all three mordants at different concentrations gave the same results.

Mangolim et al., (2014) prepared curcumin and ß-CD ICs by co-precipitation, solvent evaporation and freeze drying. The best yield of the ICs was 74% reached by coprecipitation. By these ICs, the ability of curcumin retention was increased against sunlight. In one month, 90% of the dye remained in the ICs whereas without ICs 80% remained. The effect of pH on the dye was almost the same with or without ICs. Until neutral pH, a higher absorbance was obtained (0.4) whereas as the pH was increased above 7, the absorbance

was reduced to 0.3 at pH 9. After 90 days of storage at 15°C, the ICs retained almost 100% of the dye whereas 90% remained without ICs. At 25°C of storage, there was almost the same amount of retention with or without ICs after 60 – 120 days.

S. Li et al., (2018) investigated the dyeing of ramie fabrics with curcumin in NaOH/Urea at low temperature. 0.06 – 2.4 wt.% of curcumin concentration and 7 wt.% NaOH/12 wt.% urea was used in a 1:30 liquor ratio at temperatures ranging from 5 – 80°C for 120 minutes. A K/S value of 2.36 was found for the fabric dyed with NaOH/Urea as compared to 0.53 for the fabric only dyed with water. At low temperature (10°C), the K/S value was 2.36 whereas at higher temperature (80°C), the K/S value reached 0.12. Hence, they concluded that higher temperatures degrade the dye and lead to a reduced colour. The variation of the concentration of curcumin showed an opposite effect. The higher the concentration, the higher was the K/S value. At 2.4 wt.% of curcumin, a K/S value of 6.03 was reached as compared to 0.3 wt.% of curcumin only 1.79 was determined. With 0.6% of curcumin dye, the UV protection was much higher. It reached a 64 ultraviolet protection factor (UPF) for the dyed fabric. While for the raw fabric, it was 27. This UPF value also increased with an increasing concentration of curcumin. It reached from 50 to 73 with an increasing concentration from 0.3 – 2.4 wt.%. After 4 washing cycles, the fabric maintained a washing fastness value of 4, meaning that most of the color stayed. After 12 washing cycles, it was reduced to 3.

Although there have been numerous studies on the manufacturing of curcumin and ß-CD ICs through electrospinning using solutions like ethanol, water, etc. there have been very few studies on the preparation of curcumin, ß-CD ICs in ionic liquids through dry-jet wet spinning. Coscia et al., (2018) prepared regenerated cellulose/curcumin fibers by the use of 1-Ethyl 3-Methyl imidazolium diethyl phosphate (emim DEP). This work was also the inspiration for the incorporating of curcumin and ß-CD through dry-jet wet spinning using [DBNH][OAc]. They added different concentrations of curcumin to the dope mixture, ranging from 0,1,5 and 10 wt.% with respect to 4 wt.% of cellulose/emim DEP solution. SEM imaging of the fibres revealed that the diameters of the fibres decreased with increasing winding speed. The cross section of all fibres, regardless of curcumin concentration was nearly circular. There was no effect of curcumin concentration on the fibre diameter, however, as the winding speed increased from $1.5x10^{-1}$ m/s to $4.8x10^{-1}$ m/s, the diameter of the fibres decreased from 99.2 – 51.5 μm. In terms of mechanical properties, Young's moduli, tensile strength and strain all decreased with increasing curcumin concentration. At 1 wt.% of curcumin, young's modulus was 16 GPa, tensile strength was 336 MPa and strain was 11.2%. But when the concentration increased to 10 wt.%, they reduced to 13.6 GPa, 223.2 MPa and 9.9%, respectively. Moreover, there was not a significant effect of curcumin concentration on the orientation of fibres. The orientation of fibres at all curcumin concentrations was around 0.70.

3 Research Materials and Methods

3.1 Chemicals & Materials

The used bleached kraft pulp, Enocell5 was acquired from Stora Enso Oy (pulp and paper industry company) in Finland. Chemicals like ß-Cyclodextrin (ß-CD, $C_{42}H_{70}O_{35}$, CAS: 7585-39-9, M=1134.99 g/mol, purity= ≥97%), Curcumin ($C_{21}H_{20}O_6$, CAS: 458-37-7, M= 368.39 g/mol, purity= ≥65%), 1,5-Diazabicyclo[4.3.0]non-5-ene (DBN, $C_7H_{12}N_2$, CAS: 3001-72-7, M= 124.18g/mol, purity= 98%), acetic acid (HOAc, CH_3CO_2H, CAS:64-19-7, M= 60.05 g/mol, purity= ≥99%), D-(+)-Galactose ($C_6H_{12}O_6$, CAS: 59-23-4, M=180.16g/mol, purity= ≥99%), D-(+)-Glucose ($C_6H_{12}O_6$, CAS: 50-99-7, M=180.16g/mol, purity= ≥99%), D-(+)-Xylose ($C_5H_{10}O_5$, CAS: 58-86-6, M=150.13g/mol, purity= ≥99%), Sodium Hydroxide (NaOH, CAS: 1310-73-2, M=40 g/mol, purity= ≥98%, anhydrous pellets), D-(+)-Mannose ($C_6H_{12}O_6$, CAS: 3458-28-4, M= 180g/mol, purity= ≥99.5%) and Phenol red indicator ($(C_6H_4OH)_2C_7H_4SO_3$, CAS: 143-74-8, M= 354.38g/mol, purity= ≥99.5%) were purchased from Sigma Aldrich®. Ethanol (C_2H_5OH, ETAX Aa, purity = ≥99.5%) were obtained from ANORA industries, Finland.

3.2 Ionic Liquid Preparation

In this project the ionic liquid (IL), 1,5-diazabicyclo[4.3.0]non-5-enium acetate ([DBNH][OAc]) was used. It was prepared by slowly adding an equimolar amount of acetic acid (HOAc) to the superbase 1,5-Diazabicyclo[4.3.0]non-5-ene (DBN) in a 6L reactor at 70°C. After mixing stirring was continued for an additional hour to ensure the completion of the reaction (Guizani et al., 2021).

3.3 Pulp Pretreatment

For the preparation of the dopes, Enocell5 pulp was used. Therefore, one sheet of the Enocell5 pulp was first cut into small strands and further shredded into pieces. The shreds were then milled by means of a Wiley mill M02 (mesh size 30 mm) until a fluffy mass was obtained (Sixta et al., 2015). According to the standard ISO 638:2008 (*ISO - ISO 638:2008 - Paper, Board and Pulps — Determination of Dry Matter Content — Oven-Drying Method*, 2008) in triplicate around 50 mg of the milled sample was dried in the oven Thermo Scientific HERAEUS VT 6025 overnight at 105°C to determine the dry matter content of the pulp.

3.4 Preliminary Heat-Stage Microscopy Tests

To observe the dissolution behavior of cellulose (Enocell5 pulp), curcumin and ß-CD in the IL [DBNH][OAc], different mixtures were prepared and analyzed by a Zeiss Axio Heating Stage microscope at 80°C for four minutes per trial. Each sample was prepared in triplicates. In total four mixtures were prepared, and details of their contents are given in table 1.

Table 1: Heat Stage microscopy mixtures for preliminary estimation of dissolution of curcumin and ß-CD in combination with Enocell5 in [DBNH][OAc] at 80°C.

Trial	Enocell5	[DBNH][OAc]	Curcumin	ß-CD
1	Yes	Yes	-	-
2	Yes	Yes	Yes	-
3	Yes	Yes	-	Yes
4	Yes	Yes	Yes	Yes

3.5 Spinning Dope Preparation

By the use of 2 different units two large dopes (dope 8 & 9) and 5 small dopes (dope 1-7) have been prepared. The details of the contents of each dope and the used settings are given in the Table 2.

First a calculated amount of preheated and melted IL (melted at 80°C) was poured into a kneader equipment. In case of dope 1-8 (see table 2), a calculated amount of Curcumin and/or β-CD were first added and mixed with the IL for 30 minutes to ensure a homogeneous distribution. After that, the desired amount of Enocell5 pulp was added and the mixture was kneaded for 2-3 hours at 80°C, 30 rpm under 50-70 mbar vacuum to avoid air bubbles. During kneading (every 30 min), small samples were extracted to evaluate the dissolution behavior by the heating stage microscope.

Next, the dopes were filtered at 80°C by a vertical filtration unit equipped with an y_{max} 2 metal filter (5 µm mesh) at 400 bar to remove undissolved residues. The filtered dopes were carefully collected and shaped by hand. The dopes were wrapped in clean plastic sheets and stored at 4°C in a cold room till spinning day (Guizani et al., 2021).

Table 2: Dope preparation settings. The kneading temperature was 80 °C, pressure was 50 – 70 mbar and the kneading speed was 30 rpm for all dopes.

Dope	Unit	Enocell5 (dry) (g)	Enocell5 concentration (%)*	IL [DBNH][OAc] (g)	Curcumin (g)**	ß-CD (g)***	Mixing time (hours)
1	Small unit	3.900	13	26	0.3800	-	2.5
2		3.092	10	27	0.0392	-	2.5
3		3.092	10	27	0.0392	-	2.5

4		3.092	10	27	-	0.01684	2
5		3.092	10	27	0.0392	0.06184	2
6		3.092	10	27	0.0392	0.06184	2
7		3.092	10	27	0.0392	0.06184	2
8	Large unit	159.080	10	1389	-	3.18160	2
9		315.880	13	2109	-	-	2.5

All the weights are according to the dry weight of Enocell5 with dry matter content of 97%. *For the dopes 1 and 9, 13% Enocell5 concentration was used, while the rest of the trials had 10% Enocell5. **The concentration of curcumin used for each trial was 1% according to 10% Enocell5. ***The concentration of ß-CD used in each trial was 2% as compared to Enocell5.

3.6 Rheological Analysis

The viscoelastic properties of the dopes were analysed by means of an Anton Par Physica MCR 302 Rheometer with a plate (25 mm plate diameter and 1 mm gap). The complex viscosity (η^*) and storage and loss moduli (G', G'') as a function of angular frequency (ω) were determined between 50°C to 90°C using 5°C temperature increments and a dynamic frequency sweep test from 0.01 to 100 rad/s. Under the assumption of the validity of the Cox-Merz rule the zero-shear viscosity and the crossover moduli were analysed by the use of the Cross model (Sixta et al., 2015).

3.7 Spinning Experiments

In total 2 dry-jet wet lyocell type spinning units (KS15, KS80) equipped with different spinnerets (KS80: 200 holes, 0.1 mm diameter, 0.02 mm capillary length; KS15: 1 hole, 0.1 mm diameter, 0.02 mm capillary length) from Fourné Maschinenbau GmbH have been used. Dopes 1-7 (see table 3) were spun by the use of KS15 and the dopes 8 and 9 were spun by KS80. The overall assembly of both spinning lines are almost the same, as shown in the scheme (Figure 4).

At the beginning the dopes were transferred to the cylinder, equipped with a filter (mesh 6 µm), a breaking plate, a spinneret, a temperature/pressure sensor and a heating jacket. Next the dopes were molten at around 62-72°C. The dopes were spun, stretched into an air gap (~0.5 cm) and immersed into a cold water (<11°C) bath (coagulation bath). The formed filaments were guided to a godet couple ($V_{pick\text{-}up}$) by the use of a Teflon roller, positioned in the bath. The extrusion velocity (V_e) in case of large spinning was kept constant at 5.5 cm^3/min and for monofilament spinning it was kept at 0.01

cm^3/min. The dopes were spun at draw ratio (DR = $v_{pick-up}/v_e$) 5, 8 and 11 and the maximum DRs were determined. The fibres after spinning were cut carefully with a razor blade into 10 cm pieces for analysis and into 40 mm staple length for yarn production. Next the fibers were washed at first with cold water and then three times with hot water (80°C), and dried under controlled conditions (RH= 62%; T=20°C) for fibre testing (Asaadi et al., 2018).

Table 3: Used settings of dope spinning trials.

Dopes	Type of Spinning	Water bath temperature (°C)	Extrusion speed (cm^3/min)	DR	Temperature of Spinning (°C)
1	Monofilament	5	0.01	-	66 – 90
2	Monofilament	5	0.01	5,8,11 Max: 15	65
3	Monofilament	5	0.01	-	63 - 75
4	Monofilament	5	0.01	-	65
5	Monofilament	5	0.01	-	65
6	Monofilament	5	0.01	5,8,11	62
7	Monofilament	5	0.01	5,8,11 Max: 18	62
8	Multifilament	<11	5.50	5,8,11 Max: 14	65
9	Multifilament	<11	5.50	5,8,11 Max: 14	67

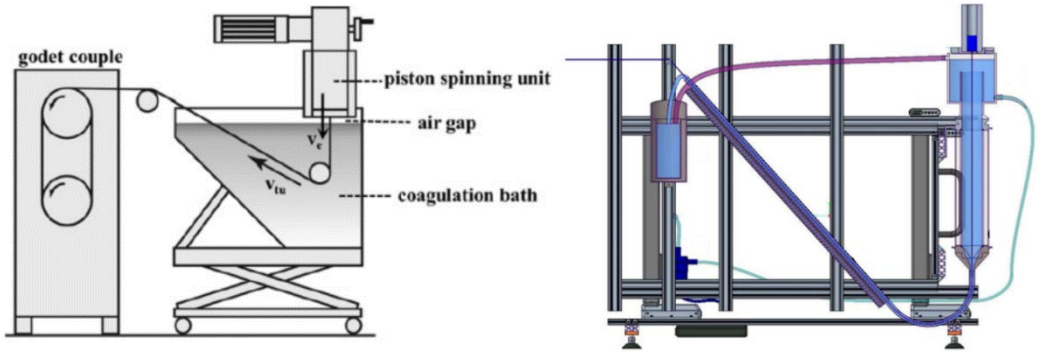

(A) **(B)**

Figure 4: Spinning line schemes. **(A)** Spinning line scheme for multifilament spinning (Sixta et al., 2015); **(B)** Spinning line scheme for monofilament spinning (Guizani et al., 2021).

3.8 Fourier Transform Infrared Spectroscopy (FTIR), Differential Scanning Calorimetry (DSC) and Thermogravimetric analysis (TGA)

The chemical structure of all the fibres was analyzed by the use of a Perkin Elmer FT-IR (ATR) equipment between 400 – 4000 cm^{-1}, by means of 30 scans with 0.5 intervals at each scan (Jia et al., 2011). Besides, the thermal

behavior of the samples was analyzed by DSC and TGA measurements using a Netzsch STA 449 F3 Jupiter & QMS 403 Aëolos Quadro device. The samples were analyzed at inert conditions under Helium, with a gas flow of 70 ml /min within a temperature range of 40 – 600°C by the use of a heating rate of 10 K/min (Awal et al., 2010).

3.9 X-ray Diffraction (XRD)

The polymer crystallinity and the crystal dimensions were determined via a SmartLab X-Ray Diffractometer from RIGAKU and calculated according to the Scherrer equation (Asaadi et al., 2018).

3.9.1 Wide Angle X-ray Scattering (WAXS)

Small pieces of fibres were placed at a sample holder and diffraction data was collected from 5° to 60° 2θ by θ/2θ settings. The diffraction data was corrected for smoothing and subtraction of air scattering and inelastic contribution as explained in the methods by (Guizani et al., 2021). Therefore, the crystallinity index (*CRI*) from a range of 9° – 50° 2θ was estimated according to eq. 1 using estimated amorphous contribution ($I_{bkg}\ (2\theta)$).

$$CRI = 100 * \frac{\int I(2\theta)\mathrm{d}2\theta - \int I_{bkg}(2\theta)\mathrm{d}2\theta}{\int I(2\theta)\mathrm{d}2\theta} \qquad (1)$$

Where, CRI = *crystallinity index (percent %)*

I_{bkg} = *background profile* (radians)

I= *total intensity* (radians)

Three pseudo-Voigt functions for $(1\bar{1}0)$, (110) and (020) for cellulose II were used to fit the background corrected profiles. Due to overlap of peaks between (110) and (020), the values of crystal dimensions were reported as average values. Additionally, Hermans orientation factor (f_{WAXD}) was estimated by eq. 2.

$$f_{WAXD} = \frac{3\cos^2\varphi_c - 1}{2} \qquad (2)$$

Where, f_{WAXD} = *Hermans orientation factor*

$\cos^2\varphi_c$ = *orientation distribution between fiber and crystallographic c-axis*

3.10 Post Spinning Dyeing

Spun standard IONCELL® fibres (dope 9) and fibres from dope 8 containing 2% ß-CD were dyed after spinning with two different solutions of the curcumin dye. In the first post spinning dyeing trial, the fibres were dyed in a solution of 1% curcumin in 2% (w/v) of NaOH solution at 100°C for one hour (S. Li et al., 2019). After dying the fibres were washed until neutral pH was maintained. However due to the instability of curcumin in basic conditions a second dyeing trial was performed with 1% curcumin in 30% (v/v) ethanol for one hour at 100°C. After the dyeing, the fibres were washed until there was no release of dye in the washing water (Peila et al., 2021) visible anymore. Next, the fibres were dried at room temperature overnight (Figure 5).

(A) **(B)**

Figure 5: Dyeing of spun fibres with curcumin. **(A)** Dyeing with 2%(v/v) NaOH and 1% curcumin solution. The first image shows the fibres after dyeing before washing. The second image is the washing water containing released dye; **(B)** Dyeing with 30%(v/v) ethanol and 1% curcumin. The first image is after the dyeing procedure and before washing. The second and third image shows the release of the dye to the washing water.

3.11 Fibre testing

According to the standard SN:41442 the mechanical properties of all fibres (samples from dopes 2,6,8 and 9) were tested with a single fibre Textechno Favigraph by Textechno Herbert Stein GmbH & Co.KG (Germany) equipment with a 70 – 150 mg pretension weight attached to the fibres in dry and wet testing. The measurements were done at 20 ± 2°C at around 65 ± 5 % relative humidity (RH). Elongation and tenacity of the fibres were tested in both dry and wet conditions. A load cell of 20 cN, a test speed of 20 mm/min and the gauge length of 20 mm were used. 15 fibres from each sample were tested.

The total cellulose orientation of the fibres was tested by first collecting three fibres of each sample of the same linear density. The fibers were attached to a glass slide and then observed at three different places by the Zeiss Axio Scope. A1 with a Tilting Compensator B. From each spot, the optical retardation value was determined. Next the polarized light retardation value was divided by fibre thickness which was determined through the linear density (cellulose density was considered as 1.5 g/cm^3). Then, the birefringence value (Δn) was calculated by using the polarized retardation value. Δn was then

divided by maximum birefringence value (0.067) for cellulose, to obtain total orientation (Moriam, et al., 2021b).

3.12 Scanning Electron Microscopy (SEM)

The Fibre morphology was determined by the use of a Zeiss Sigma VP microscope at 3keV operating voltage. The fibre samples were cryo-fractured with liquid nitrogen, followed by drying overnight at 105°C. The dried cryo-fractured fibres were then transferred from the cracked end onto the sample holder. The samples were then sputtered with Gold/Palladium particles (4 nm) (Kaniz, 2022).

3.13 Quantification of ß-CD

The amount of ß-CD available in fibres was estimated through the method of (Dehabadi et al., 2014) using only Phenol Red for the quantification. Fibres produced from dope 8 (2% ß-CD and 10% Enocell5) and standard IONCELL® fibres (dope 9) were used in this method. However, the method was modified for estimation in spun fibres (in this case) as follows. The fibres were ground into a fine powder using Wiley mini-mill 475-A using a mesh size of 30 mm. The ground fibres were then processed in analogy to Dehabadi et al., (2014). Before each drying cycle, the ground fibres were recovered with pre-weighed filter paper (25 mm pore size) through vacuum filtration. Each drying cycle was performed overnight at 105°C. The weight fraction (w*) of ß-CD fixed onto the fibre were calculated as mean of triplicates according to eq. 3.

$$w^* = \frac{n_{dye} \times M_{ß-CD} \times 100}{m_{fibre}} \qquad (3)$$

Where, w^*% = weight fraction of ß-CD fixed onto the fibre (percent: %)
n_{dye} = Moles of Phenol Red dyestuff used calculated through spectroscopic measurements (moles)
$M_{ß-CD}$ = Molecular weight of ß-CD (grams/moles: g/mol)
m_{fibre} = mass of fibres initially used (grams: g)

3.14 Washing Fastness & Brightness Testing

Fibres from dopes 2,7,8, 9 and post spinning dyed fibres were measured for brightness using the GretagMacbeth Spectroscan equipment. Each sample was measured in triplicates and a white surface was used as a reference and the averaged CIE LAB values were analysed.

The washing fastness of the fibres from dope samples (2,7 and post spinning dyed fibres) were tested according to the European Standard ISO 106-C06,

1997 (*EN ISO 105-C06*, 2016). The sample preparation was proceeded according to the standard and A1S test was performed on all the samples. The samples were washed with a washing liquor for 30 minutes in Linitest Original Hanau washer at 40°C and rinsed with 40°C water two times (each for 1 minute). Afterwards, the colors of the fibres were compared with grey scale for assessing change in color (ISO Recommendation R105/I/Part 2, British Standard B.S. 2662:1961) and the change in multi-fibre fabric staining with grey scales for assessing staining (ISO Recommendation R105/I/Part 3, British Standard B.S. 2663:1961) as per standard procedures.

4 Results

4.1 Preliminary Heat-Stage Microscopy

Before dope preparation, a preliminary dissolution test was performed by means of the heat-stage microscope at 80°C, to observe the dissolution behavior of the components (curcumin, cyclodextrin) in [DBNH][OAc] in combination with Enocell5. The results are shown in figure 6.

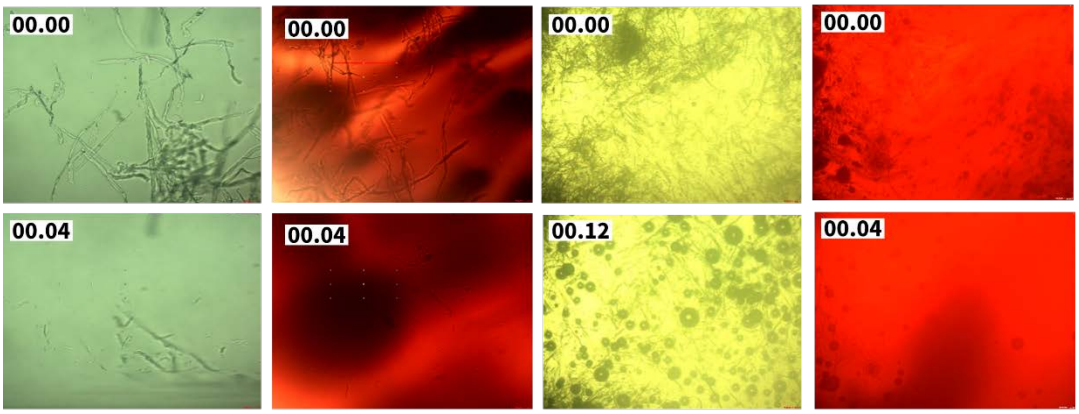

Figure 6: Dissolution behavior of curcumin and ß-CD in [DBNH][OAc] in combination with Enocell5. The text in white displays the time stamps in minutes, all images were taken at 10x magnification. **(A)** Trial 1: Enocell5 and [DBNH][OAc], **(B)** Trial 2: Enocell5, [DBNH][OAc] with curcumin, **(C)** Trial 3: Enocell5, [DBNH][OAc] with ß-CD, **(D)** Trial 4: Enocell5, [DBNH][OAc], curcumin and ß-CD.

Enocell5 pulp dissolved within 4 minutes at 80°C (Figure 6A). The same phenomenon was observed for trial 2 and 4 (Figure 6B, D). However, there was a slight delay in dissolution of the Enocell5 fibres in the presence of ß-CD (Figure 6C). As we can see from the figure, the dissolution took longer (around 12 minutes). There was also a strange appearance of a lot of air bubbles when ß-CD was involved. However, in trial 4, the pulp dissolved after 4 minutes and there was also some appearance of air bubbles. Overall, it was possible to dissolve all mixtures by means of [DBNH][OAc] to the same extent as standard pulp (Sixta et al., 2015).

4.2 Spinning Dope Preparation

The dopes for each trial were prepared according to Sixta et al., (2015) by means of the settings and contents mentioned in Table 2 (in methodology section). For standard IONCELL® dope (dope 9), Enocell5 was dissolved completely within 3 hours of kneading and every 30 minutes samples were extracted to observe the dissolution behavior by the use of the heating-stage microscope. As confirmed by the heating-stage microscopy investigations

(Figure 7), most of the enocell5 pulp was dissolved within the first hour, but the kneading was continued for two hours to ensure complete homogeneity. The same procedure was implemented for the mixtures ß-CD/Enocell5 (dope 8), curcumin/Enocell5 (dope 2) and ß-CD/curcumin/Enocell5 (dope 6). The standard IONCELL® dope after kneading had a smooth appearance, a honey like color and an elastic, caramel like consistency. The same consistence was observed in dopes with added curcumin and ß-CD. However, the dopes with curcumin had a red coloration (see Figure 7).

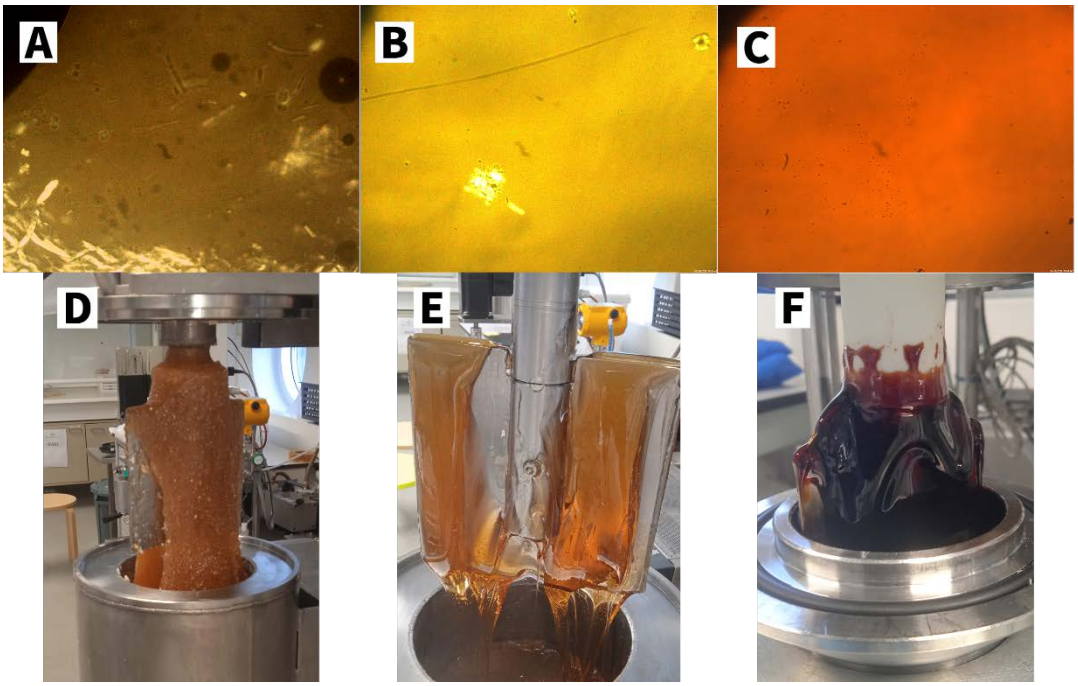

Figure 7: Illustration of dope preparation and dissolution behavior via microscope images (10x magnification) after 1 hour of kneading. Dissolution of Enocell5 standard IONCELL® dope (**(A)**, dope 9), 2% ß-CD/20% Enocell5 dope (**(B)**, dope 8) and 1% curcumin/2% ß-CD/10% Enocell5 mixture (**(C)**, dope 2). Illustration of standard IONCELL® dope (**(D)**, dope 2), 2% ß-CD/20% Enocell5 dope (**(E)**, dope 8) and 1% curcumin/2% ß-CD/10% Enocell5 mixture (**(F)**, dope 2).

4.3 Rheological Properties

Even though, the rheological properties of all dope trials were measured, but for the sake of simplification, the data of dope 2 (1% curcumin), 6 (1% curcumin/2% ß-CD/10% Enocell5), 8 (2% ß-CD/10% Enocell5 dope) and 9 (standard IONCELL® dope) are presented as representatives here.

The elasticity (solid properties) of a material is defined by the storage modulus (*G'*), which shows the material`s ability to store energy elastically, and the loss modulus (*G"*), the ability to dissipate stress. On the other hand, flow properties are displayed in terms of complex viscosity (η^*) (Lu et al., 2019). Figure 3 displays the trends of storage and loss moduli, and complex

viscosity versus angular frequency (ω) from an oscillation test at 80°C. In case of moduli (Figure 8A), the moduli for all three dopes (2,6,8) displayed similar behavior. An overlap of trends can be observed. Both storage and loss moduli of samples, increased with increasing angular frequency. The cross over point where the trendline of storage and loss moduli met are similar and in total for each dope 1 cross over point was found. In terms of complex viscosity (Figure 8B), it was the same for all samples (dope 2,6,8). The complex viscosity decreased with increasing angular frequency. All the trends are quite close to the trend of the standard IONCELL® dope.

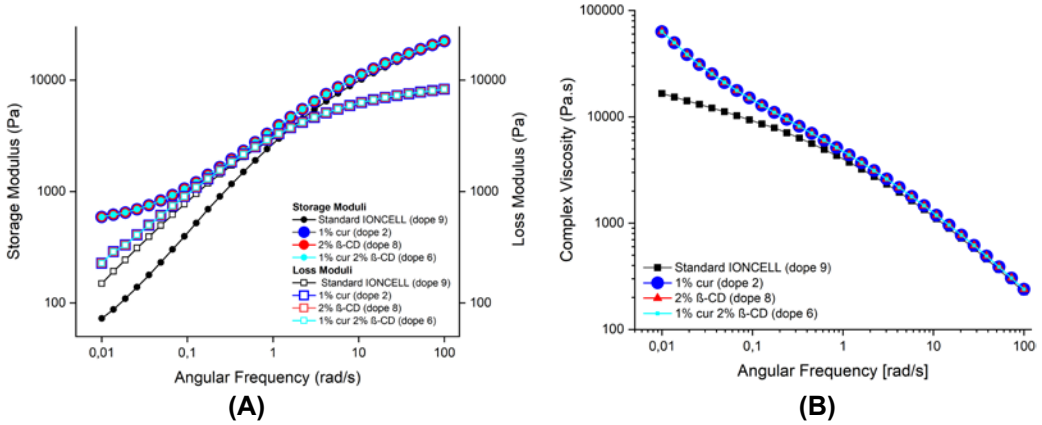

(A) **(B)**

Figure 8: Rheological measurements of dope 2 (1% curcumin), 6 (1% curcumin/2% ß-CD/10% Enocell5) and 8 (2% ß-CD/10% Enocell5 dope) vs. standard IONCELL® dope (dope 9). **(A)** Storage and loss moduli of dopes against angular frequency measured at 80°C. **(B)** Complex viscosity against angular frequency measured at 80°C.

As cellulose is a long chain molecule, in solution it creates more entanglements because of which individual cellulose chains can't move freely leading to enhanced zero-shear viscosity of the solution. In this case, the concentration of Enocell5 varies between the dope 9 (13%) and the rest of the dopes (10%). This affects the zero-shear viscosity and moduli of the viscoelastic solutions. Despite this difference in concentration the complex viscosity trends of the dopes 2,6 and 8 only differ at low angular frequencies from the standard IONCELL® dope. The moduli of the dopes form 1 COP, close to the COP of the standard IONCELL® dope (Kaniz, 2022). Normally, as cellulose concentration increases, zero-shear viscosity also increases and the viscoelastic solution becomes more viscous (Haward et al., 2012). However, in this case, a different trend is shown. Despite the reduction in cellulose consistency (dopes 2,6,8: 10% enocell5) compared to dope 9 (13% enocell5), the complex viscosity almost stays the same, and at lower angular frequencies a rise in complex viscosity is illustrated. Consequently, an addition of ß-CD and/or curcumin results in dopes with increased complex viscosities compared to the standard IONCELL® dope. This might by caused by an integration of the additives to the cellulose chains, leading to restrictions in the mobility of the

polymer. However, this effect was bridged by the reduction of the Enocell5 content to 10% (Sharma & Satapathy, 2021).

4.4 Spinning of the Fibres

In analogy to the literature dopes 2,3,6,7,8 and 9 were successfully spun (Sixta et al., 2015). Dopes 3 and 7 were repetitions of dope 2 and 6, respectively. Therefore, as mentioned earlier, dopes 2,6,8 and 9 will be the main subjects of discussion. The fibres from dope 9 were standard IONCELL® fibres. These fibres were spun using multifilament spinning (200 holes) and around 90 g of fibres were collected at DR 5,8 and 11. These fibres looked off-white in color (Figure 9A). The remaining dopes were spun by the use of the monofilament unit (1 hole). Fibres from dope 2,3 were yellow in color and felt strong on touch. These fibres only contained 1% curcumin. On the other hand, the fibres from dope 6 and 8 both contained 2% ß-CD appeared shiny and lustrous. The fibres from dope 6 which also had 1% curcumin along with ß-CD appeared strong yellow with a shiny finish. Table 6 lists the successful dopes, their maximum DRs and the DRs at which fibers were collected.

Even though, there has not been previous works done in incorporating curcumin and ß-CD by means of dry-jet wet spinning, there are well established research works for incorporating ß-CD and curcumin by electrospinning. In this work, 1% curcumin and 2% of ß-CD have been utilized according to the work done by Coscia et al., (2018). Coscia et al., utilized various concentrations of curcumin (0 - 10%) in combination with cellulose and the IL, 1-Ethyl 3-Methyl Imidazolium diethyl phosphate (Emim DEP). According to their results, the concentration of curcumin didn't make much of a difference and the properties of fibres were the same for 1% curcumin or 10% curcumin. Therefore, in our work, keeping in mind the minimalistic approach of use of chemicals, we decided to utilize 1% of curcumin with regard to the cellulose weight. Additionally, the color of fibres from dopes 2 and 6 (both contained 1% curcumin) was also bright yellow, what is in line with the results of Coscia et al.

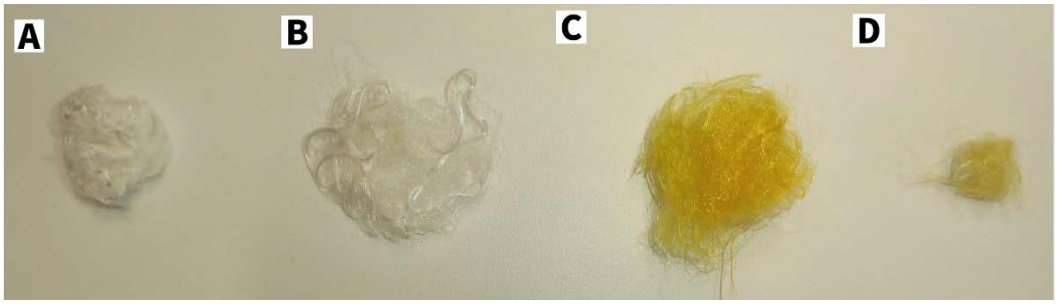

Figure 9: Appearance of fibres after spinning, washing and drying. **(A)** Fibres spun from dope 9: standard IONCELL® fibres; **(B)** fibres spun from dope 8: 2% ß-CD/10% Enocell5; **(C)** fibres spun from dope 6: 1% curcumin/2% ß-CD/10% Enocell5; **(D)** fibres spun from dope 2: 1% curcumin/10% Enocell5.

Table 6: Successful dopes and collected DRs.

Dope	Contents of dope	Type of spinning	Maximum DR	DRs collected
2	1% curcumin, 10% Enocell5	Monofilament	15	5, 8, 11
6	1% curcumin, 2% ß-CD, 10% Enocell5	Monofilament	18	5, 8, 11
8	2% ß-CD, 10% Enocell5	Multifilament	14	5, 8, 11
9	13% Enocell5	Multifilament	14	5, 8, 11

Cyclodextrins (CDs) are able to encapsulate a variety of molecules due to their unique structure. Even though, the stoichiometry of most encapsulates (inclusion complexes) are usually 1:1 i.e., one molecule of CD encapsulating one other molecule, other versions, like 1:2 (1 CD molecule : 2 other molecules), 2:1 (2 CD molecules : 1 other molecule) and 2:2 (2 CD molecules : 2 other molecules) are possible. The composition depends on the amount of CDs and the interactions of the molecules (Kfoury et al., 2016). However, the formed structure of the CD – dye – CD complex wasn`t verified within this MSc thesis.

4.5 Fibre Testing

Fibre orientation and the elongation of the fibres produced at DR 5, 11 and 8 were measured (Figure 10). The orientation value was measured by birefringence, which is the determination of the optical properties of a material having a refractive index. In general, the increase in total orientation of fibres is only seen until a certain draw ratio, where after that at a certain draw ratio the fibres no longer orient and a detrimental effect on the structure of the fibre due to cellulose chain slippage might occur (Mortimer & Péguy, 1996). With regard to the spinning, an increase in DR and consequently an increase of the extensional stress in the air gap, results in an increased alignment of the cellulose chains along the filament axis and leads to an increase in tenacity and total orientation (Asaadi et al., 2018).

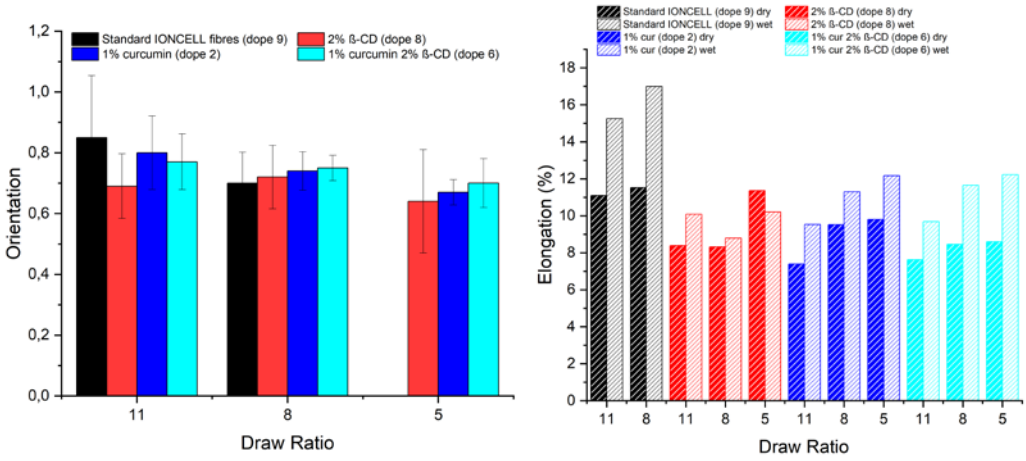

Figure 10: Orientation and elongation of fibres at different draw ratios. **(A)** Orientation of fibres from dope 2,6,8 and 9; **(B)** elongation of fibres from dope 2,6,8, and 9, shaded bars are for dry elongation and unshaded for wet elongation.

The elongation of fibres depends on the orientation of the fibers and on the applied draw ratio during fiber production. The elongation (both wet and dry) for dope 6 containing both ß-CD and curcumin is between the elongation of the dopes 2 and 8. The elongation values ranged between 8 – 11% for all fibre samples which is in alignment with the results achieved by Elsayed et al., (2021). Elsayed et al., reported an elongation value of around 11% for fibres spun with [DBNH][OAc]. Elongation is an important mechanical property for diverse textile applications. There is a widespread for the values of elongation at break for different DRs (Figure 10B). However, a decrease of DR results in an increase of elongation. The average tenacity of all fibre samples at break is around 3.5 – 4.5 (cN/dtex) (Figure 11). This matches with the results of (Suzuki et al., 2021). The maximum of Tenacity was reached in most cases by DR8. Only in the presence of ß-CD the maximum Tenacity was achieved by DR11. In general fibers, which contained ß-CD showed a reduced elongation compared to standard fibers. The tenacity values are in the range of the standard fibers produced at DR11, however, have not reached the tenacity of DR8 standard fibers. Besides, all of the dopes, which contained curcumin showed as well reduced elongation values compared to the standard dope. Tenacity values are close to the standard dope values, but in the presence of ß-CD the reached stress values are shifted to the dope, which only contains ß-CD (Figure 10: red). However, the fiber properties might have been compromised by the cellulose dope consistency, as the standard fibres were produced by dope 9, a 13% enocell5 dope and all of the other fibers by the use of dopes with a 10% enocell5 consistence. A higher cellulose concentration increases orientation and in turn increases other mechanical properties of the fibre (Sixta et al., 2015). The elongation (E_{max}), dry and wet average tenacity along with fibre orientation are given in table 7.

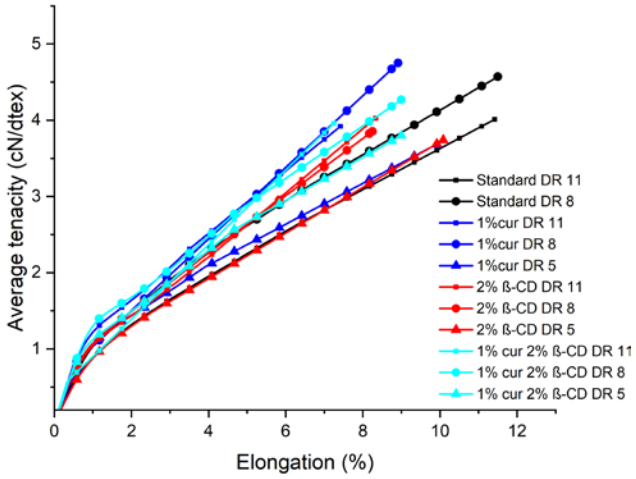

Figure 11: Comparison of elongation vs. dry average tenacity of fibres from dopes 2 (Blue),6 (Cyan),8 (Red) and 9 (Black).

Table 7: Mechanical properties of spun fibres at different DRs.

Fibres from dope samples	**DR**	***E_{max} (%)**		**Average Tenacity (cN/tex)**		**Orientation**
		Dry	**Wet**	**Dry**	**Wet**	
2	5	9.8 ± 2.3	12.2 ± 3.9	36.8 ± 9.3	34.1 ± 10.1	0.67 ± 0.04
	8	8.4 ± 1.9	11.6 ± 3.4	43.5 ± 19.2	29.8 ± 8.2	0.74 ± 0.06
	11	7.6 ± 1.8	9.6 ± 2.2	43.6 ± 5.4	35.7 ± 7.8	0.80 ± 0.12
6	5	8.6 ± 2.2	12.2 ± 3.9	34.5 ± 9.5	34.1 ± 10.1	0.70 ± 0.08
	8	8.4 ± 1.9	11.6 ± 3.4	43.5 ± 19.2	29.8 ± 8.2	0.75 ± 0.04
	11	7.6 ± 1.8	9.6 ± 2.2	43.6 ± 5.4	35.7 ± 7.8	0.77 ± 0.09
8	5	11.3 ± 1.9	10.2 ± 3.8	37.6 ± 7.3	38.1 ± 5.4	0.64 ± 0.17
	8	8.3 ± 2.3	8.7 ± 3.4	38.5 ± 8.8	23.2 ± 8.1	0.72 ± 0.10
	11	8.3 ± 1.6	10.0 ± 1.1	40.2 ± 6.3	42.7 ± 2.5	0.69 ± 0.10
9	8	11.5 ± 2.7	16.9 ± 2.3	45.7 ± 5.8	44.9 ± 3.6	0.70 ± 0.10

	11	11.0 ± 3.6	15.2 ± 3.6	38.8 ± 9.9	44.8 ± 11.0	0.85 ± 0.20

*Elongation (E_{max})

4.6 FTIR and DSC/ TGA

FTIR spectra of the starting materials. curcumin. Enocell5 and ß-CD along with the fibers produced by the dopes 2,6,8 and 9 are shown in Figure 12A. The general trend for all fibers is similar. Enocell5 which is basically cellulose, has characteristic broad peak at 3332cm^{-1} which is the O-H stretching vibration. The peak at 2916cm^{-1} is the CH_2 stretching. Peaks around 1436/1375 are the deformation of CH2/CH bonds. Whereas 1078cm^{-1} has a strong peak which represents C-O-C stretching vibrations (Sun et al., 2021). ß-CD consists of glucose units and consequently it shows the same pattern as Enocell5. Looking at the characteristic peaks of ß-CD, it has a similar broad peak in the region 3300 - 3400cm^{-1} which also corresponds to OH group stretching just like the Enocell5. Another peak at 2929cm^{-1} is for symmetrical or asymmetrical CH group stretching. Similarly, a peak at 1082cm^{-1} might be for CH and C-O stretching vibrations (Mohan et al., 2012). Curcumin represented by yellow curve (Figure 12A), shows a small sharp peak at 3508cm^{-1} correlating with OH group vibrations. Even though there are many characteristic peaks for curcumin, which can be seen from the curves, the marked ones (dashed lines) are the ones which are found in fibres (from curcumin, ß-CD and Enocell5). Peak at 1272cm^{-1} are the enol C-O peaks. Finally, the sharp peak at 1023cm^{-1} represents C-O-C stretching (Kolev et al., 2005).

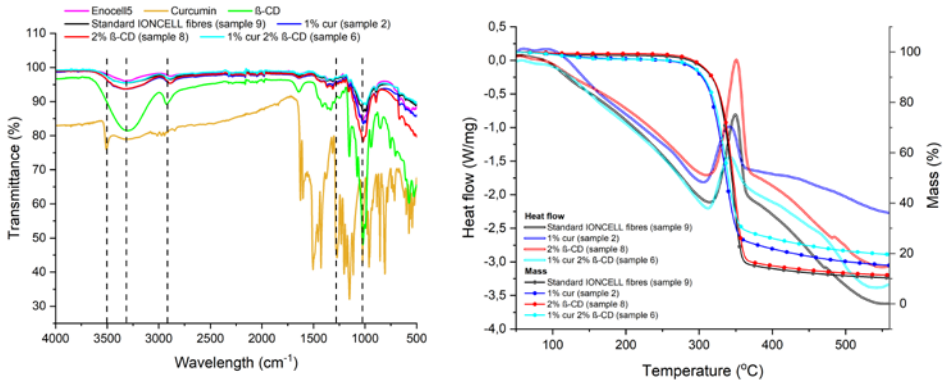

(A) **(B)**

Figure 12: FTIR, DSC and TGA thermograms. **(A)** FTIR spectra of Enocell5, curcumin, ß-CD and fibers spun from dope samples 2,6,8 and 9; **(B)** DSC thermogram with TGA curves of fibres spun from dope samples 2,6,8 and 9.

However, The Figure 12A is just an estimation as the structure of ß-CD and Enocell5 are quite similar and might mask the presence of ß-CD (Mohan et al., 2012). Peaks at 1150 and 1621cm^{-1}, found in this case, are C-O-C vibrations of ß-CD, benzene ring vibrations of curcumin and C=O stretching

vibrations of curcumin. The characteristic peaks of curcumin display a shift to higher numbers caused by interactions of the benzene ring of curcumin with ß-CD (Mangolim et al., 2014).

Differential Scanning Calorimetery (DSC) is an excellent tool which can provide useful qualitative insights on the physico-chemical state of the molecules involving complex formation and how the complexes interact with the host-guest components (Yadav et al., 2009). At the beginning some differences are shown. (Figure 12B). After ~150°C the heat flows start to decrease until around 300°C. From here onwards until 380°C, the peaks rise indicates an endothermic transition reaction, until one point and then rapidly fall leading to further fall in heat flow until the end. Celebioglu & Uyar (2020) showed in their work that there was an endothermic peak at 177°C which indicates the melting of curcumin. However, in our case, this endothermic peak was around 250°C in case of 1% curcumin, indicating. For dope 9 (standard IONCELL® fibres), there was no peak found, which indicates the presence of no curcumin. Also, the broad small peak between 30 – 140°C, indicates water loss. This is in accordance with the work of Celebioglu & Uyar (2019). This broad peak could also mask the initial melting peak of curcumin. However, in the cyclodextrin complexes, the melting of the guest molecules is not possible to detect with DSC because during the complex formation they are separated from each other and cannot form crystals (Narayanan et al., 2017).

Thermogravimetric analysis (TGA) is a technique which provides information about the thermal stability of a material and it's volatile components by monitoring the changes in mass as a result of heating at a constant rate (Rajisha et al., 2011). The TGA thermogram (Figure 12B – dotted lines) shows a weight loss at around 300°C for all samples which is in accordance with the DSC curves. The weight losses of dope 6 (1% curcumin and 2% ß-CD) and 2 (1% curcumin) and the weight losses of standard dope and dope 8 are similar. The similarity of standard dope and dope 8 is caused by the molecule structure. ß-CD as well as enocell5 consists of glucose units. Moreover, the weight loss of dope 2 (1% curcumin) is initially completely overlapping with the weight loss of dope 6 (1% and 2% ß-CD), however, differs at the end of the transition reaction at inert conditions (helium atmosphere). This is in accordance with the work of Sharma & Satapathy (2021), but the transition reaction started slightly at lower temperatures for dopes 2 and 8. The increased weight fraction in later parts of the thermograms in case of dope 6 (1% curcumin and 2% CD), might lead to the assumption that there are interactions between the curcumin molecule and the ß-CD molecules. This might be an indication of microcapsules formed between curcumin and ß-CD (Rezaei & Nasirpuri, 2018).

4.7 XRD results

The crystallinity and the crystal dimensions of components in solid state can be determined using XRD. The shift or reduction in diffraction peaks indicate the formation of amorphous structures which can give insights about the formation of inclusion complexes. However. these diffractogram patterns vary according to the method utilized for inclusion complex formation. e.g. freeze drying, kneading, etc. (Kfoury et al., 2016). Figure 13 shows the diffractograms of the samples under consideration. The figure shows three major reflexes for all samples at around 12°, 20-23° and around 35°. There are some other minor reflexes found at around 30° and 40° (French, 2014). Even though the reflexes appear at the same angles for all samples, they vary in intensity. The highest intensities can be observed for dope 8 and 2 fibres. On the other hand. the intensity for dope 6 and 9 were almost close, but less than those from the others. The labels in the plot depict the major crystal planes of cellulose II polymorphs (Gong et al., 2017).

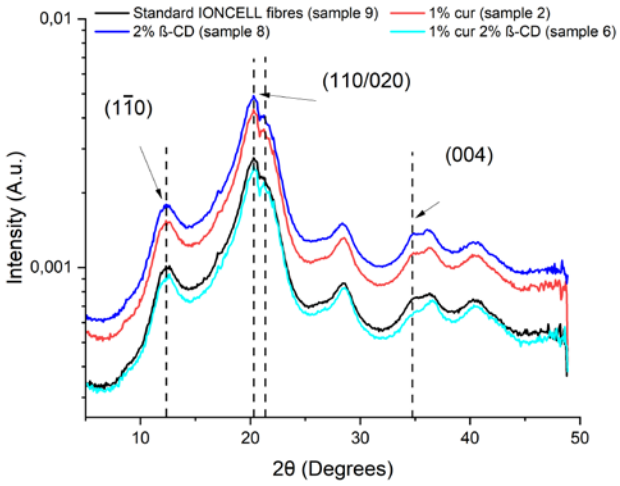

Figure 13: XRD patterns of fibers indicating cellulose II crystal planes.

Curcumin in its raw powdered form shows a sharp reflex at 15°. However, in this case, no peak was found. The structure of curcumin in raw form is crystalline. On the other hand, ß-CD has a semi-crystalline structure. Therefore, these reflexes might be shifted and hidden by cellulose II (in dope 2 and 6) (Rezaei & Nasirpuri, 2018). Moreover, the appearance of the reflexes and the intensity of curcumin including fibres (dope 2 and 6) are exactly the same as shown by the work of Coscia et al., (2018). As mentioned earlier. curcumin in its raw form is crystalline but when it is incorporated into the cellulose structure or when it is in the form of inclusion complexes, it changes to amorphous forms. The explanation for this is that when inclusion complexes are formed, the guest molecules cannot make their own crystalline aggregates as they are separated by the cavity of ß-CD molecules (Celebioglu & Uyar, 2020). Since the pattern for all the fibre samples is the same, it can be assumed that the additives are hidden by the intensive peaks of cellulose II.

Another aspect about curcumin is that it is hydrophobic and can make a non-covalent bond with the hydrophobic structure of ß-CD. This also predicts a good ability to form inclusion complexes (Giordano et al., 2001). Nonetheless, there are same diffraction patterns observed for fibres where there is no curcumin or guest molecules involved. For example in the case of dope 8 and 9, the reflexes in this case might be relating to the reflexes of cellulose II crystals. The crystallinity index (*CRI*) and fibre dimensions of the samples were analysed and are discussed in the SEM section.

4.8 Post-Spinning Dyeing of Fibres

Curcumin has a unique diketone functionality and exists in two tautomeric forms: a keto form and enol form (Lykidou et al., 2021). This confirmation makes it soluble in alcohols but insoluble in water (Tsatsaroni et al., 1998). Also, curcumin has a lower affinity to cellulosic fibers which also makes it difficult to be used as a dye for such fibres. For this purpose, usually some pre-treatments for instance mordants are needed to facilitate the dyeing process. However, many of these mordants are metallic components which are toxic (Li et al., 2018). Due to the toxicity of these components, within this work dyeing without the utilization of additives was pursued.

Fibres from dope 8 and 9 were tested for dyeing with 1% curcumin after spinning to compare the effects of traditional dyeing and incorporating of curcumin by ß-CD. For post spinning dyeing trials, two different methods were tested. First dyeing by the use of NaOH 2% (w/v) with 1% curcumin and second dyeing by 30% ethanol (v/v) and 1% curcumin was utilized. The details are described in the methodology section.

A solution of NaOH helps to dissolve cellulose by breaking the intramolecular hydrogen bonds and helps in regenerating cellulose. There have been previous works where it was shown that NaOH with urea aqueous solution at low temperatures causes cellulose-based fabrics to swell, hence NaOH can be used for a solvent to facilitate dyeing. as demonstrated by (Li et al., 2018). In the work of Peila et al., (2021), where they also utilized 2% NaOH as one of the liquors of dyeing. They report similar results with cellulose acetate and cotton fabrics. This could be due to the unavailability or low availability of intrinsic groups of cellulose interacting with the dye molecules.

Moreover, under acidic and neutral conditions curcumin exhibits a yellow color because it is in its keto form whereas in alkaline conditions or pH > 8, it changes color to red which is due to its keto form (Figure 1A methodology section). This alkalinity must be neutralized before washing, usually with H_2SO_4. This neutralization step helps to gap the distance between the cellulose molecules in a way that the dye molecule entrapped between cellulose molecules are fixed in their position, hence stay in the cellulose structure (Zhou & Tang, 2016).

On the other hand, in case of solvents like ethanol, it appears that the fibres are dyed much better. But since the pH of the 30% ethanol (v/v) solution in water has a pH close to neutral pH (Deleebeeck et al., 2021), it is also not a very effective dyeing liquor, but it is much better than the NaOH dyeing trial. This is in accordance with the work of Hasan et al., (2014), where they dyed cotton with curcumin and the maximum dye uptake was at pH 7 and at alkaline pH the dye converts to its enol form hence the dye uptake was not successful.

The first dyeing method performed with 2% NaOH was not successful. Most of the dye was removed during the washing procedure and the fibres were almost the same in appearance and color as before (Figure 15A). This was caused by the instability of the dye at alkaline conditions. Therefore, another method of dyeing by the utilization of 30% ethanol was tested. This method was tested using fibres produced by dope 8 and 9. The fibres after dyeing with ethanol appeared bright yellow for both fibre samples (Figure 14A,B), even though some color was lost while washing the samples. In this study, the dyeing stability was further tested with washing fastness testing, which is discussed ahead.

4.9 Washing Fastness & Brightness Testing

The color of the fibre samples prepared from dope 2,6,8,9 and post spinning dyed fibres were measured by the determination of the CIE LAB color space. The values are given in Table 8.

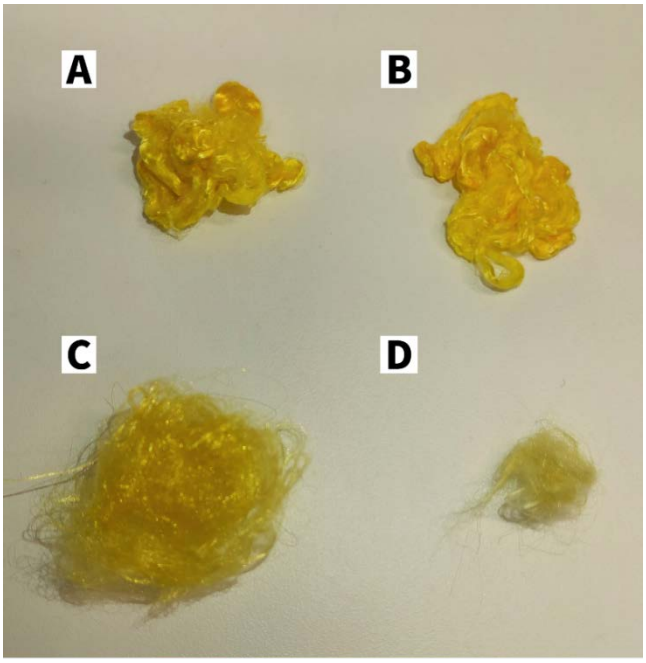

Figure 14: Comparison of spin dyeing and traditional dyeing by the use of EtOH. **(A)** Fibres produced by dope 9 (standard IONCELL® fibres) dyed with 1% curcumin in EtOH; **(B)** Fibres

produced by dope 8 (2% ß-CD) dyed with 1% curcumin after spinning in EtOH; **(C)** fibres spun from dope 6 (1% curcumin. 2% ß-CD); **(D)** fibres spun from dope 2 (1% curcumin).

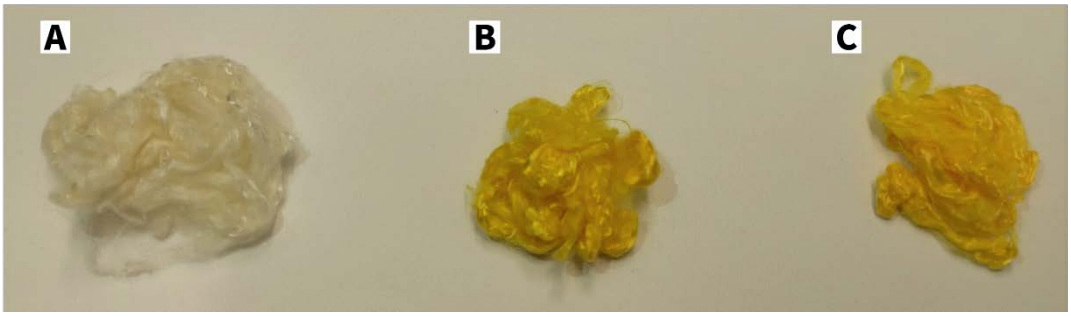

Figure 15: Comparison of fibers produced by spin dyeing and dyeing by the utilization of NaOH and EtOH. **(A)** Fibres produced by dope 9 (standard IONCELL® fibres) dyed with 2% NaOH and 1% curcumin after spinning; **(B)** Fibres produced by dope 8 (2% ß-CD) dyed with 1% curcumin in 30% ethanol (v/v) after spinning; **(C)** Fibres produced by dope 9 (standard IONCELL® fibres) dyed with 1% curcumin in 30% ethanol (v/v).

Table 8: Brightness measurements of fibre samples.

Fibre samples from dope	Contents of sample	CIE LAB			Color
		L	A	B	
2	1% curcumin	77.13	1.08	50.86	Yellow
6	1% curcumin, 2% ß-CD	69.16	3.72	57.21	Yellow
8	2% ß-CD	78.29	-0.01	7.93	Beige
9	13% Enocell 5	86.09	2.48	8.52	Beige
Post dyed fibres from dope 9 (2% NaOH)	13% Enocell 5	73.25	-0.10	17.92	Beige
Post dyed fibres from dope 9 (30% ethanol)	13% Enocell 5	76.01	7.72	77.25	Yellow
Post dyed fibres from dope 8 (30% ethanol)	2% ß-CD	74.53	9.15	80.13	Yellow

Samples were tested for washing fastness for 30 minutes at 40°C (A1S test according to European Standard ISO 106-C06. 1997 (*EN ISO 105-C06*. 2016). The dye of the fibres prepared from dope 2 and 6 (spin dyeing) retained and the fibres prepared from dopes 8 and 9 which were dyed after spinning with 30% ethanol and 1% curcumin lost their yellow color. It can be assumed from these results that the fibres containing the dye during the spinning were more stable in holding the dye than the fibres dyed after the

spinning (Figure 15). Besides the color of the fibres prepared from dopes 8 and 9 which were dyed after the spinning changed from yellow to red partly (Figure 16A & B). In order to assess the release of the dye and staining affect on fabric, a multi-fibre fabric[1] as a reference was used. The color change and staining grading is given in table 9.

Table 9: Results of the washing fastness test illustrating the color change and staining grading.

Fibres from dope samples	Contents of the sample	Dyeing (with 1% curcumin)	Color change grading	Multi-fibre fabric staining grading					
				1	2	3	4	5	6
2	1% curcumin	Spin dyeing	4	5	5	5	5	5	5
6	1% curcumin, 2% ß-CD	Spin dyeing	4	5	5	5	5	4/5	5
8	2% ß-CD	Post spinning, with 30% ethanol	1	5	5	5	3/4	3	5
9	13% Enocell5	Post spinning, with 30% ethanol	1	4/5	5	5	4	3	5

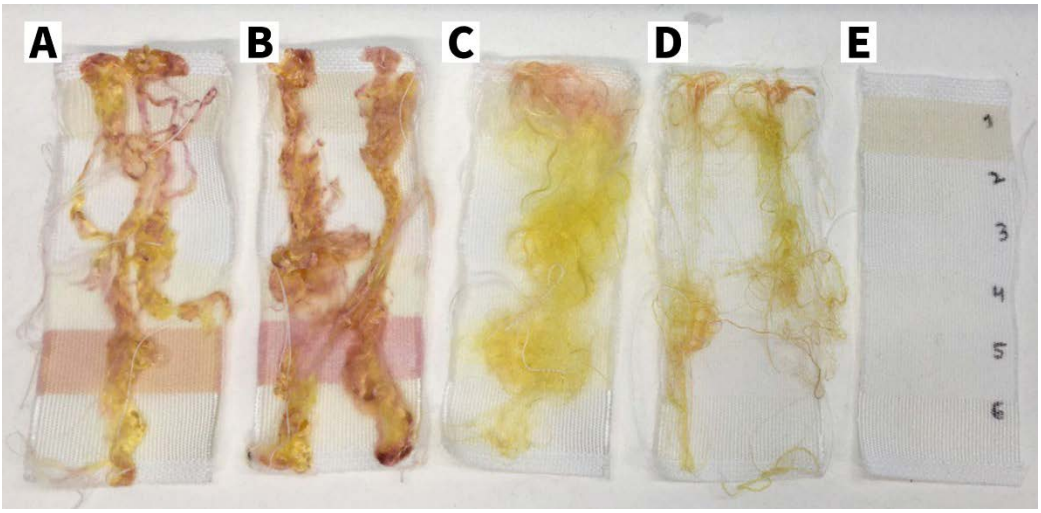

Figure 16: Photograph of the washing fastness in combination with a multi-fibre fabric. **(A)** fibres prepared from dope 9 dyed after spinning with 30% ethanol and 1% curcumin; **(B)** fibres prepared from dope 8 dyed after spinning with 30% ethanol and 1% curcumin; **(C)** fibres prepared from dope 6 containing 1% curcumin and 2% ß-CD; **(D)** fibres prepared from dope 2 containing 1% curcumin; **(E)** multi-fibre reference fabric.

The color fastness reached good values (4 and 5) in terms of fibre samples produced from dope 2 and 6 (spin dyeing), as no staining and almost no color change was observed. However, it has to be mentioned, that less amounts of

[1] Composition of the multi-fibre fabric layers: 1-Wool; 2- Acrylic; 3- Polyester; 4- Polyamide; 5- Bleached cotton and 6- Diacetate

fibres produced from dope 2 were utilized for testing as recommended by the standard due to the unavailability of sufficient amounts of fibres. Even though there was a very small amount of dye released within the detergent (Figure 17A), the difference between fibers produced with and without ß-CD was not very pronounced. Also, in case of fabric staining, 4/5 grading was assigned to fabric layer 5 (bleached cotton) in the case of fibres produced from dope sample 6. This might be caused also by the difference in the amount of fibres. If the amounts were the same, it is very likely that the effect in both cases (fibers produced from dope 2 and 6) might be the same. In the 5th layer (bleached cotton) of the multi-fibre fabric (in the case of post spinning dyed fibres) a red discoloration is shown. This effect also slightly varies due to the difference in the used amount of samples. Even though almost same color change and staining grading was assigned to these two samples, the effect of color retention in the presence of ß-CD can be detected through the color release during washing (Figure 17B).

The red color appearance can be attributed to the presence of alkaline elements in the detergent. Curcumin in contact with alkaline components changes the structure to its enol form and hence the color to red.

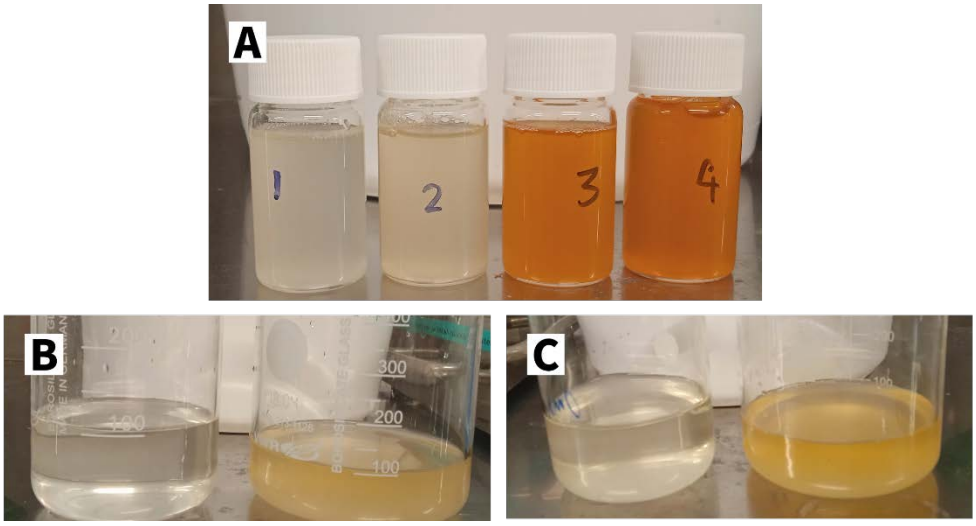

Figure 17: Comparison of dye release during rinsing of samples post washing. **(A)** Detergent collected after washing (**1-** fibre sample produced from dope 2; **2-** fibre sample produced from dope 6; **3-** fibre sample produced from dope 8 dyed with 30% ethanol and 1% curcumin post spinning; **4-** fibre sample produced from dope 9 dyed with 30% ethanol and 1% curcumin post spinning); **(B-left)** second round of rinsing water collected by post washing of fibre sample produced from dope 8 dyed with 30% ethanol and 1% curcumin post spinning; **(B-right)** first round of rinsing water collected by post washing of fibre sample produced from dope 8 dyed with 30% ethanol and 1% curcumin post spinning; **(C-left)** second round of rinsing water collected from post washing for fibre sample produced from dope 9 dyed with 30% ethanol and 1% curcumin post spinning; (**C-right)** first round of rinsing water collected from post washing for fibre sample produced from dope 9 dyed with 30% ethanol and 1% curcumin post spinning.

4.10 Fibre morphology

Figure 12 shows the cross-section and surface images of the fibres. It can be seen from the cross-section that all fibres looked similar compared to the standard IONCELL® fibres (Figure 18A). Fibrillar bodies are displayed by the cross-section images of the fibres. Their outer appearances are also mostly smooth except in the case of fibres where curcumin or ß-CD was added which show some bumps on the surface of the fibres. However. this might be also caused by the coating of the fibres for SEM analysis.

Elsayed et al., (2021) described the fibres prepared with [DBNH][OAc] as having fibrillar internal appearance while smooth outer surface. Moreover, as the DR increases, the coagulation time decreases. This leads to higher orientation and smoother fibres (Zhu et al., 2016). Crystallite size along with crystallinity index (*CRI*) measured through WAXS are given in Table 10. The CRI for fibres from dope 2 and 9 are the same, whereas for dope 6 and 8 the CRIs are a little bit higher compared to the standard fibers (dope 9). This means that the introduction of ß-CD has an effect on the mechanical properties of the fibre.

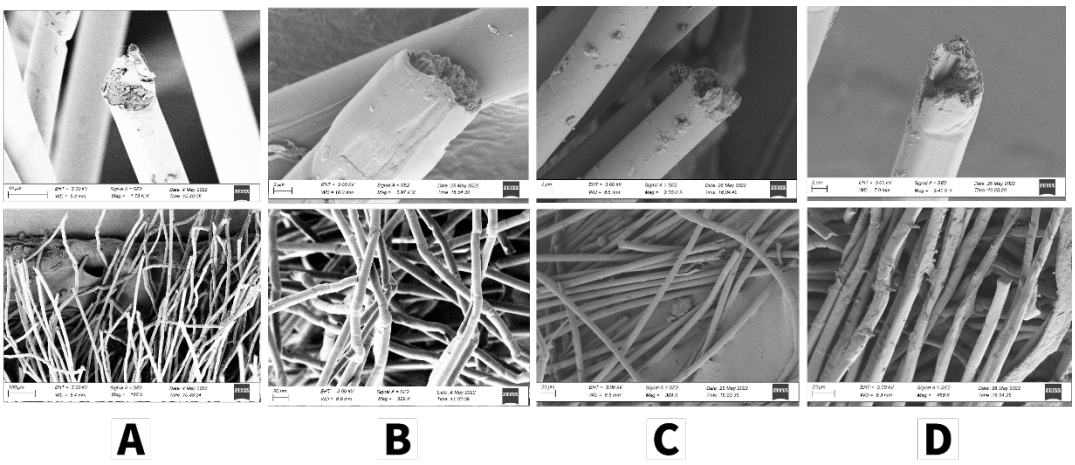

Figure 18: Fibre morphology captured through SEM at various magnifications 1.73K – 329K X). All fibres were produced by the use of DR8. The tope line shows cross section of fibres whereas the bottom line shows appearance of fibres in general. **(A)** Fibres produced from dope 9 (Standard IONCELL® fibres); **(B)** fibres produced from dope 8 (2% ß-CD. 10% Enocell5); **(C)** fibres produced from dope 6 (1% curcumin. 2% ß-CD); **(D)** fibres produced from dope 2 (1% curcumin. 10% Enocell5).

Crystallinity is the measure of the structural order of a material which means the measurement or estimation of crystalline or amorphous regions in a material. Crystallinity of cellulose is described in terms of crystallinity index (*CRI*) (Refaat, 2012). The addition of curcumin doesn't significantly affect the crystallinity of cellulose fibres. Coscia et al., (2018) confirmed the same results in their research. On the other hand, the increase in crystallinity is attributed to the addition of ß-CD (Sharma & Satapathy, 2021).

Table 10: Crystallite size and crystallinity index of fibres. Crystallite sizes are given for three crystal planes ($1\bar{1}0$), (110) and (020) of the cellulose II polymorph.

Fibre samples from dope	Contents of the sample	Crystallite size (Å)			Crystallinity Index (CRI) (%)
		$(1\bar{1}0)$	(110)	(020)	
2	1% curcumin	38.6 ± 0.7	34.8 ± 0.1	37.3 ± 0.5	73.5 ± 1.3
6	1% curcumin, 2% ß-CD	41.4 ± 1.0	35.5 ± 0.1	35.8 ± 0.2	79.1 ± 0.7
8	2% ß-CD	39.6 ± 1.0	35.0 ± 0.2	36.3 ± 0.1	76.3 ± 0.8
9	13% Enocell5	38.5 ± 1.7	34.9 ± 0.9	37.3 ± 0.4	73.3 ± 2.6

4.11 Quantification of ß-CD

Generally, to find the amount of fixed ß-CD onto textile/fibre by gravimetric estimation i.e. by measuring the weight of the sample material before and after treatment with ß-CD is possible. However, this method is not accurate enough (Grechin et al., 2016). Phenolic dyes like Phenolphthalein and Phenol Red are favorable to indicate quantitative amount of ß-CD fixed onto fibres. Phenol red in the presence of cyclodextrins changes its color from red to yellow. There are some studies on general quantification of cyclodextrins in textiles like the works of Grechin et al., (2016) and Bereck, (2010). Apart from these, there are no established studies for the quantification of cyclodextrins fixed on fibers. In the method of Dehabadi et al., (2014), phenol red was used as a guest molecule to make inclusion complexes with cyclodextrins and then washed with ethanol and alkaline water. Phenol red is insoluble in water and hence it is first dissolved with ethanol and then pH is raised to 11. The unadsorbed dye molecules are washed with ethanol and as the samples are immersed in alkaline water, the unfixed guest molecules are released from the cavities of the cyclodextrin molecule. This can be observed by a slight pink color change (Figure 19B). This is also confirmed by colorimetric measurements with the presence of a peak at 559 nm (Figure 20A).

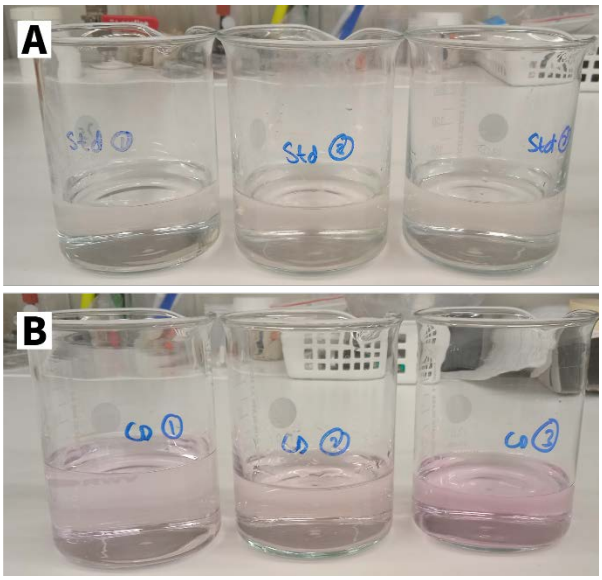

Figure 19: Color change observed during washing with alkaline water (pH=11). **(A)** No color change was observed in fibres produced from dope 9 (standard IONCELL fibres); **(B)** slight pink color observed in fibres produced from dope 8 (2% ß-CD).

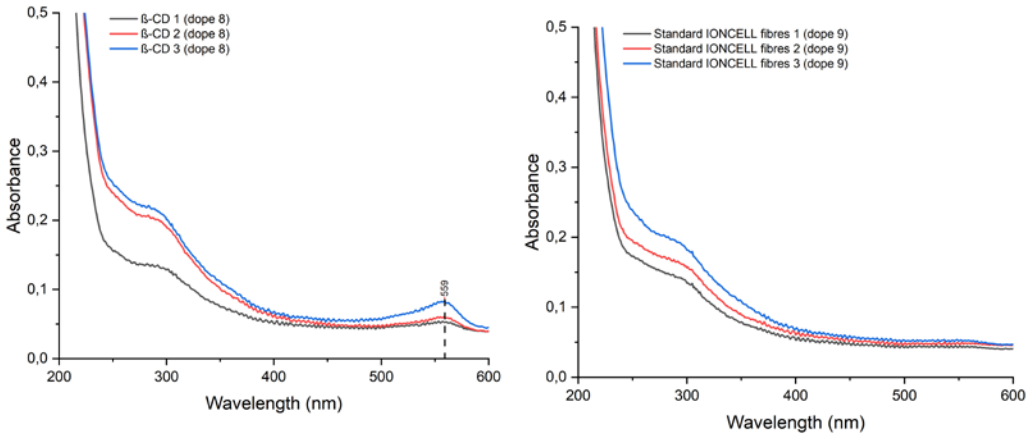

(A) **(B)**

Figure 20: Illustration of extracted Phenol red from fibres produced from dope 8 and 9. Determination of the concentration through peak estimation at 559 nm. **(A)** Peak estimation for fibres produced from dope 8 (containing 2% ß-CD); **(B)** Peak estimation for fibres produced from dope 9 (standard IONCELL® fibres).

Figure 20 shows the presence and absence of peaks at 559 nm from fibres with ß-CD and without ß-CD determined via UV/Vis spectroscopy. The peak can be seen in all three samples of fibres produced from dope 8 which contained ß-CD (Figure 20 A) while no peaks at 559nm were seen in fibres produced from dope 9 which contained no ß-CD and were simply standard IONCELL® fibres (Figure 20B). These peaks helped to determine the concentration of ß-CD fixed onto the fibres and their accessibility to make inclusion complexes (Table 11). The intensities of the peak located at 559 nm

were determined and the concentrations calculated (see table 11) by the use of the calibration curve of Phenol Red shown in Figure 21.

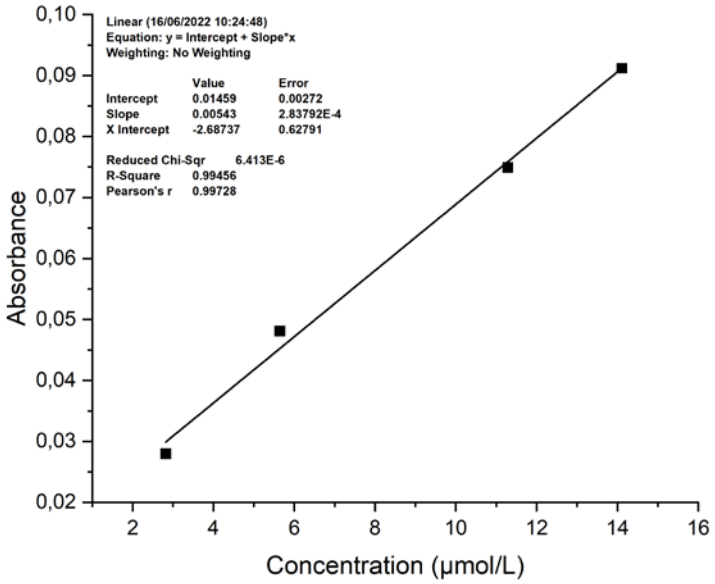

Figure 21: Calibration curve for Phenol Red solutions (pH=11).

Even though this method was relatively easy to follow (as per instructions) for a coating of cyclodextrin on a cotton fabric, however this wasn't the case for our fibre samples. In the case of fibre samples, the fibre samples had to be grinded to make sure that the extraction procedure was homogenous throughout the entire fibre sample and each drying cycle was made overnight to ensure complete removal of moisture which can affect the measurements. 2% of ß-CD was added into the dope mixture and this dope was turned into fibers by spinning. 2% was added to establish the formation of a 2:1 geometry in combination with curcumin. 1 molecule of Curcumin might be trapped by 2 molecules of ß-CD. However, the final structure was not verified. The molecules arrange themselves in different ways by hydrophilic and/or hydrophobic interactions.

Table 7: Quantification of ß-CD fixed onto the fibres and the amount accessible for encapsulation.

Sample (from dope 8)	Contents of the sample	Amount of ß-CD originally used (g)[1]	Amount of Enocell 5 originally used (g)	Amount of used fibers for determination of ß-CD in (g)	w.*(%)[2]
1	2% ß-CD	0.06184	159.08	1.0955	0.131
2	2% ß-CD	0.06184	159.08	1.0875	0.088
3	2% ß-CD	0.06184	159.08	1.0459	0.173
Average					0.119 ± 0.03

[1] This is the amount of ß-CD added into the dope mixture according to the dry mass of Enocell5. [2] w.* is the weight fraction of ß-CD fixed onto the fibre.

Considering that ß-CD and the guest molecule (Phenol red) makes an inclusion complex in 1:1 geometry, only ~0.12% of ß-CD was fixed onto the fibres. The rest of the amount of ß-CD that was initially added into the dope might have only been on the surface of the fibres and must have been washed away during spinning or when the fibres were washed after spinning. Also, as a general rule, in most cases, only a part of added cyclodextrins will be able to make inclusion complexes because of the unfavorable arrangements, possible polymerization of steric hinderance between molecules (Grechin et al., 2016).

The values are in accordance with the results of Dehabadi et al., (2014). This method works for fibres which doesn't already have a guest molecule included into the fibres with cyclodextrin. However, if there's already a guest molecule added (in the case of fibres produced from dopes 2 and 6, which contained 1% curcumin), this method will be unable to quantify the accessibility. For those samples, probably some other qualitative or quantitative methods are needed.

5 Summary/Conclusions

In this research work we explored the potential of IONCELL® technology to prepare curcumin functionalized fibres through dry jet-wet spinning. The main part of the research focused on using ß-CD for incorporating curcumin and dyeing the fibres by spin dyeing. The possibility of formed ICs were analyzed through various techniques like FTIR, DSC, XRD, TGA and SEM. The research also compares traditional dyeing after the spinning with spin dyeing as a sustainable alternative. Bright yellow fibres after spinning were obtained at DR 5,11 and 8. The fibres had strong mechanical properties almost similar to standard IONCELL® fibres. The spin dyed fibers retained the dye more than traditional dyed fibers, as confirmed by washing fastness tests. The amount of ß-CD fixed onto the fibers was determined by UV/Vis spectroscopy using Phenol red as a guest molecule.

This work opened up a new possibility to produce functional fibers by the use of ß-CD by means of the IONCELL® process. The IONCELL® process is a sustainable process for textile manufacturing. Now by the outcome of this work, new fibres with modified properties have been generated. However, more studies are needed for testing the stability (light/storage) of curcumin while being encapsulated by ß-CD in the IONCELL® fibres. Another important aspect is the evaluation of the biodegradability of the new IONCELL® fibre and performing a life cycle analysis of these fibres.

References

Ammayappan, L., & Jeyakodi Moses, J. (2009). Study of antimicrobial activity of aloevera, chitosan, and curcumin on cotton, wool, and rabbit hair. *Fibers and Polymers 2009 10:2*, *10*(2), 161–166. https://doi.org/10.1007/S12221-009-0161-2

Arias, M. J. L., Coderch, L., Martí, M., Alonso, C., Carmona, O. G., Carmona, C. G., & Maesta, F. (2018). Vehiculation of active principles as away to create smart and biofunctional textiles. *Materials*, *11*(11). https://doi.org/10.3390/ma11112152

Asaadi, S., Hummel, M., Ahvenainen, P., Gubitosi, M., Olsson, U., & Sixta, H. (2018). Structural analysis of Ioncell-F fibres from birch wood. *Carbohydrate Polymers*, *181*(September 2017), 893–901. https://doi.org/10.1016/j.carbpol.2017.11.062

Asaadi, S., Kakko, T., King, A. W. T., Kilpeläinen, I., Hummel, M., & Sixta, H. (2018). High-Performance Acetylated Ioncell-F Fibers with Low Degree of Substitution. *ACS Sustainable Chemistry and Engineering*, *6*(7), 9418–9426. https://doi.org/10.1021/acssuschemeng.8b01768

Awal, A., Ghosh, S. B., & Sain, M. (2010). Thermal properties and spectral characterization of wood pulp reinforced bio-composite fibers. *Journal of Thermal Analysis and Calorimetry*, *99*(2), 695–701. https://doi.org/10.1007/s10973-009-0100-x

Benjamin, A., Tawiah, B., & Asinyo, B. K. (2016). Advances in spun-dyeing of regenerated cellulose fibres. *International Journal of Management, Information Technology and Engineering*, *4*(2), 65–80. www.bestjournals.in

Bereck, A. (2010). Cyclodextrins in textile finishing: Fixation and analysis. *Advanced Materials Research*, *93–94*, 1–4. https://doi.org/10.4028/www.scientific.net/AMR.93-94.1

Bezerra, F. M., Lis, M. J., Firmino, H. B., Da Silva, J. G. D., Valle, R. D. C. S. C., Valle, J. A. B., Scacchetti, F. A. P., & Tessaro, A. L. (2020). The role of β-cyclodextrin in the textile industry-review. *Molecules*, *25*(16). https://doi.org/10.3390/molecules25163624

Bojana, B. P., & Marica, S. (2019). Microencapsulation technology and applications in added-value functional textiles. *Physical Sciences Reviews*, *1*(1), 1–27. https://doi.org/10.1515/psr-2015-0003

Celebioglu, A., & Uyar, T. (2019). Fast Dissolving Oral Drug Delivery System Based on Electrospun Nanofibrous Webs of Cyclodextrin/Ibuprofen Inclusion Complex Nanofibers. *Molecular Pharmaceutics*, *16*(10), 4387–4398. https://doi.org/10.1021/ACS.MOLPHARMACEUT.9B00798/SUPPL_FILE/MP9B00798_SI_002.AVI

Chang, H. T., Lin, C. Y., Hsu, L. S., & Chang, S. T. (2021). Thermal degradation of linalool-chemotype cinnamomum osmophloeum leaf essential oil and its stabilization by microencapsulation with β-cyclodextrin. *Molecules*, *26*(2). https://doi.org/10.3390/molecules26020409

Cireli, A., & Yurdakul, B. (2006). Application of cyclodextrin to the textile dyeing and washing processes. *Journal of Applied Polymer Science*, *100*(1), 208–218. https://doi.org/10.1002/app.22863

Coscia, M. G., Bhardwaj, J., Singh, N., Santonicola, M. G., Richardson, R., Thakur, V. K., & Rahatekar, S. (2018). Manufacturing & characterization of regenerated cellulose/curcumin based sustainable composites fibers spun from environmentally benign solvents. *Industrial Crops and Products*,

111(September 2017), 536–543. https://doi.org/10.1016/j.indcrop.2017.09.041
Cramer, F. D., Freudenberg, K. D., & Plieninger, H. D. (1951). *Verfahren zur Herstellung von Einschlussverbindungen physiologisch wirksamer organischer Verbindungen* (Patent No. DE895769C). https://patents.google.com/patent/DE895769C/de
Dehabadi, V. A., Buschmann, H. J., & Gutmann, J. S. (2014). Spectrophotometric estimation of the accessible inclusion sites of β-cyclodextrin fixed on cotton fabrics using phenolic dyestuffs. *Analytical Methods*, *6*(10), 3382–3387. https://doi.org/10.1039/c4ay00293h
Deleebeeck, L., Snedden, A., Nagy, D., Rozikov, M., Heering, A., Bastkowski, F., Leito, I., Quendera, R., Cabral, V., & Stoica, D. (2021). *and Acetonitrile , and Their Mixtures with Water*. 1–16.
Elsayed, S., Hellsten, S., Guizani, C., Witos, J., Rissanen, M., Rantamäki, A. H., Varis, P., Wiedmer, S. K., & Sixta, H. (2020). Recycling of Superbase-Based Ionic Liquid Solvents for the Production of Textile-Grade Regenerated Cellulose Fibers in the Lyocell Process. *ACS Sustainable Chemistry and Engineering*, *8*(37), 14217–14227. https://doi.org/10.1021/acssuschemeng.0c05330
Elsayed, S., Hummel, M., Sawada, D., Guizani, C., Rissanen, M., & Sixta, H. (2021). Superbase-based protic ionic liquids for cellulose filament spinning. *Cellulose*, *28*(1), 533–547. https://doi.org/10.1007/s10570-020-03505-y
Elsayed, S., Viard, B., Guizani, C., Hellsten, S., Witos, J., & Sixta, H. (2020). Limitations of Cellulose Dissolution and Fiber Spinning in the Lyocell Process Using [mTBDH][OAc] and [DBNH][OAc] Solvents. *Industrial and Engineering Chemistry Research*, *59*(45), 20211–20220. https://doi.org/10.1021/acs.iecr.0c04283
EN ISO 105-C06, (2016) (testimony of Suomen Standardisoimisliitto).
French, A. D. (2014). Idealized powder diffraction patterns for cellulose polymorphs. *Cellulose*, *21*(2), 885–896. https://doi.org/10.1007/S10570-013-0030-4/FIGURES/5
Giordano, F., Novak, C., & Moyano, J. R. (2001). Thermal analysis of cyclodextrins and their inclusion compounds. *Thermochimica Acta*, *380*(2), 123–151. https://doi.org/10.1016/S0040-6031(01)00665-7
Gong, J., Li, J., Xu, J., Xiang, Z., & Mo, L. (2017). Research on cellulose nanocrystals produced from cellulose sources with various polymorphs. *RSC Advances*, *7*(53), 33486–33493. https://doi.org/10.1039/c7ra06222b
Grechin, A. G., Buschmann, H. J., & Schollmeyer, E. (2007). Quantification of Cyclodextrins Fixed onto Cellulose Fibers. *Textile Research Journal*, *77*(3), 161–164. https://doi.org/10.1177/0040517507078063
Guizani, C., Larkiala, S., Moriam, K., Sawada, D., Elsayed, S., Rantasalo, S., Hummel, M., & Sixta, H. (2021). Air gap spinning of a cellulose solution in [DBNH][OAc] ionic liquid with a novel vertically arranged spinning bath to simulate a closed loop operation in the Ioncell® process. *Journal of Applied Polymer Science*, *138*(5), 1–14. https://doi.org/10.1002/app.49787
Guizani, C., Nieminen, K., Rissanen, M., Larkiala, S., Hummel, M., & Sixta, H. (2020). New insights into the air gap conditioning effects during the dry-jet wet spinning of an ionic liquid-cellulose solution. *Cellulose*, *27*(9), 4931–4948. https://doi.org/10.1007/S10570-020-03115-8/FIGURES/10
Gupta, S. C., Patchva, S., Koh, W., & Aggarwal, B. B. (2012). Discovery of curcumin, a component of golden spice, and its miraculous biological activities. *Clinical and Experimental Pharmacology and Physiology*, *39*(3),

283–299. https://doi.org/10.1111/J.1440-1681.2011.05648.X
Haji, A. (2020). Functional finishing of textiles with β-cyclodextrin. *Frontiers of Textile Materials: Polymers, Nanomaterials, Enzymes, and Advanced Modification Techniques*, 87–116. https://doi.org/10.1002/9781119620396.ch4
Hasan, M. M., Nayem, K. A., Yousuf, A., & Azim, M. A. (2014). *Dyeing of Cotton and Silk Fabric with Purified Natural Curcumin Dye*.
Hauru, L. K. J., Hummel, M., Michud, A., & Sixta, H. (2014). Dry jet-wet spinning of strong cellulose filaments from ionic liquid solution. *Cellulose*, *21*(6), 4471–4481. https://doi.org/10.1007/S10570-014-0414-0/TABLES/1
Haward, S. J., Sharma, V., Butts, C. P., McKinley, G. H., & Rahatekar, S. S. (2012). Shear and extensional rheology of cellulose/ionic liquid solutions. *Biomacromolecules*, *13*(5), 1688–1699. https://doi.org/10.1021/bm300407q
Heinze, T., El Seoud, O. A., & Koschella, A. (2018). *Cellulose Derivatives*. Springer International Publishing. https://doi.org/10.1007/978-3-319-73168-1
Hummel, M., Michud, A., Ma, Y., Roselli, A., Stepan, A., Hellstén, S., Asaadi, S., & Sixta, H. (2018). High-performance Lignocellulosic Fibers Spun from Ionic Liquid Solution. *Cellulose Science and Technology*, 341–370. https://doi.org/10.1002/9781119217619.ch14
Hummel, M., Michud, A., Tanttu, M., Asaadi, S., Ma, Y., Hauru, L. K. J., Parviainen, A., King, A. W. T., Kilpeläinen, I., & Sixta, H. (2014). Ionic liquids for the production of man-made cellulosic fibers: Opportunities and challenges. *Advances in Polymer Science*, *271*, 133–168. https://doi.org/10.1007/12_2015_307
ISO - ISO 638:2008 - Paper, board and pulps — Determination of dry matter content — Oven-drying method, (2008). https://www.iso.org/standard/42267.html
Jia, N., Li, S. M., Ma, M. G., Zhu, J. F., & Sun, R. C. (2011). Synthesis and characterization of cellulose-silica composite fiber in ethanol/water mixed solvents. *BioResources*, *6*(2), 1186–1195.
Jiang, X., Bai, Y., Chen, X., & Liu, W. (2020). A review on raw materials, commercial production and properties of lyocell fiber. In *Journal of Bioresources and Bioproducts* (Vol. 5, Issue 1, pp. 16–25). Elsevier. https://doi.org/10.1016/J.JOBAB.2020.03.002
Kaniz, M. (2022). *Modification of Ioncell spinning technology to increase fiber toughness and create a water- repellent surface* [Aalto University]. https://aaltodoc.aalto.fi/bitstream/handle/123456789/114137/isbn9789526407661.pdf?sequence=1&isAllowed=y
Kfoury, M., Hădărugă, N. G., Hădărugă, D. I., & Fourmentin, S. (2016). Cyclodextrins as encapsulation material for flavors and aroma. In *Encapsulations*. https://doi.org/10.1016/b978-0-12-804307-3.00004-1
Kolev, T. M., Velcheva, E. A., Stamboliyska, B. A., & Spiteller, M. (2005). DFT and experimental studies of the structure and vibrational spectra of curcumin. *International Journal of Quantum Chemistry*, *102*(6), 1069–1079. https://doi.org/10.1002/QUA.20469
Lestari, M. L. A. D., & Indrayanto, G. (2014). Curcumin. *Profiles of Drug Substances, Excipients, and Related Methodology*, *39*, 113–204. https://doi.org/10.1016/B978-0-12-800173-8.00003-9
Lewin, M. (2006). *Handbook of Fiber Chemistry* (3rd ed.). Taylor and Francis Ltd.
Li, M., Zhu, L., Zhang, T., Liu, B., Du, L., & Jin, Y. (2017). Pulmonary delivery of tea tree oil-β-cyclodextrin inclusion complexes. *Journal of Pharmacy and Pharmacology*, *69*, 1458–1467.

Li, S., Lu, M., Hu, R., Tang, T., Hou, K., & Liu, Y. (2018). Dyeing Ramie Fabrics With Curcumin in NaOH/Urea Solution at Low Temperature: *Https://Doi.Org/10.1177/0887302X18798133*, *37*(1), 66–79. https://doi.org/10.1177/0887302X18798133

Li, S., Lu, M., Hu, R., Tang, T., Hou, K., & Liu, Y. (2019). Dyeing Ramie Fabrics With Curcumin in NaOH/Urea Solution at Low Temperature. *Clothing and Textiles Research Journal*, *31*(1), 66–79.

Lu, Y., Qian, X., Xie, W., Zhang, W., Huang, J., & Wu, D. (2019). Rheology of the sesame oil-in-water emulsions stabilized by cellulose nanofibers. *Food Hydrocolloids*, *94*(February), 114–127. https://doi.org/10.1016/j.foodhyd.2019.03.001

Lykidou, S., Pashou, M., Vouvoudi, E., & Nikolaidis, N. (2021). Study on the Dyeing Properties of Curcumin on Natural and Synthetic Fibers and Antioxidant and Antibacterial Activities. *Fibers and Polymers*, *22*(12), 3336–3342. https://doi.org/10.1007/s12221-021-0412-4

Malcolm, R., & M., I. (2007). Cellulose: Molecular and Structural Biology. In *Cellulose: Molecular and Structural Biology*. Springer Netherlands. https://doi.org/10.1007/978-1-4020-5380-1

Mangolim, C. S., Moriwaki, C., Nogueira, A. C., Sato, F., Baesso, M. L., Neto, A. M., & Matioli, G. (2014). Curcumin-β-cyclodextrin inclusion complex: stability, solubility, characterisation by FT-IR, FT-Raman, X-ray diffraction and photoacoustic spectroscopy, and food application. *Food Chemistry*, *153*, 361–370. https://doi.org/10.1016/J.FOODCHEM.2013.12.067

Mangolim, C. S., Moriwaki, C., Nogueira, A. C., Sato, F., Baesso, M. L., Neto, A. M., & Matioli, G. (2014). Curcumin-β-cyclodextrin inclusion complex: stability, solubility, characterisation by FT-IR, FT-Raman, X-ray diffraction and photoacoustic spectroscopy, and food application. *Food Chemistry*, *153*, 361–370. https://doi.org/10.1016/J.FOODCHEM.2013.12.067

Maurer, R. J., Sax, A. F., & Ribitsch, V. (2013). Moleular simulation of surface reorganization and wetting in crystalline cellulose I and II. *Cellulose*, *20*(1), 25–42. https://doi.org/10.1007/S10570-012-9835-9

McKeen, L. W. (2012). Environmentally Friendly Polymers. *Permeability Properties of Plastics and Elastomers*, 287–304. https://doi.org/10.1016/B978-1-4377-3469-0.10013-X

Mikkola, J. P., Kirilin, A., Tuuf, J. C., Pranovich, A., Holmbom, B., Kustov, L. M., Murzin, D. Y., & Salmi, T. (2007). Ultrasound enhancement of cellulose processing in ionic liquids: From dissolution towards functionalization. *Green Chemistry*, *9*(11), 1229–1237. https://doi.org/10.1039/b708533h

Minns, J. W., & Khan, A. (2002). α-cyclodextrin-I3- host-guest complex in aqueous solution: Theoretical and experimental studies. *Journal of Physical Chemistry A*, *106*(26), 6421–6425. https://doi.org/10.1021/jp020628r

Mohan, P. R. K., Sreelakshmi, G., Muraleedharan, C. V., & Joseph, R. (2012). Water soluble complexes of curcumin with cyclodextrins: Characterization by FT-Raman spectroscopy. *Vibrational Spectroscopy*, *62*, 77–84. https://doi.org/10.1016/j.vibspec.2012.05.002

Moriam, K., Sawada, D., Nieminen, K., Hummel, M., Ma, Y., Rissanen, M., & Sixta, H. (2021). Towards regenerated cellulose fibers with high toughness. *Cellulose*, *28*(15), 9547–9566. https://doi.org/10.1007/s10570-021-04134-9

Morin-Crini, N., Fourmentin, S., Fenyvesi, É., Lichtfouse, E., Torri, G., Fourmentin, M., & Crini, G. (2021). 130 years of cyclodextrin discovery for health, food, agriculture, and the industry: a review. *Environmental Chemistry Letters 2021 19:3*, *19*(3), 2581–2617.

https://doi.org/10.1007/S10311-020-01156-W
Mortimer, S. A., & Péguy, A. A. (1996). The formation of structure in the spinning and coagulation of lyocell fibres. *Cellulose Chemistry and Technology*, *30*(1–2), 117–132.
Narayanan, G., Boy, R., Gupta, B. S., & Tonelli, A. E. (2017). Analytical techniques for characterizing cyclodextrins and their inclusion complexes with large and small molecular weight guest molecules. *Polymer Testing*, *62*, 402–439. https://doi.org/10.1016/j.polymertesting.2017.07.023
Paramera, E. I., Konteles, S. J., & Karathanos, V. T. (2011). Stability and release properties of curcumin encapsulated in Saccharomyces cerevisiae, β-cyclodextrin and modified starch. *Food Chemistry*, *125*(3), 913–922. https://doi.org/10.1016/j.foodchem.2010.09.071
Patel, B. H. (2011). Natural dyes. In *Handbook of Textile and Industrial Dyeing: Principles, Processes and Types of Dyes* (Vol. 1). Woodhead Publishing Limited. https://doi.org/10.1533/9780857093974.2.395
Peila, R., Varesano, A., Vineis, C., Bobba, V., Bobba, J., Piriou, A., & Barazzotto, M. (2021). Fabric dyeing with colorimetric pH-responsive colours. *Colorat*, *137*, 123–133.
Pfennig, A. (1995). Kirk-Othmer Encyclopedia of Chemical Technology, 4th Ed., Vol. 10. M. Howe-Grant (Editor). John Wiley & Sons, New York 1993. 1022 S. mit zahir. Abb. und Tab., geb., £ 185.00. In *Chemie Ingenieur Technik* (Vol. 67, Issue 3). John Wiley & Sons, Ltd. https://doi.org/10.1002/CITE.330670323
Podgornik, B. B., Šandric, S., & Kert, M. (2021). Microencapsulation for functional textile coatings with emphasis on biodegradability—a systematic review. *Coatings*, *11*(11). https://doi.org/10.3390/coatings11111371
Raduly, F. M., Raditoiu, V., Raditoiu, A., & Purcar, V. (2021). Curcumin: Modern Applications for a Versatile Additive. *Coatings 2021, Vol. 11, Page 519*, *11*(5), 519. https://doi.org/10.3390/COATINGS11050519
Rajisha, K. R., Deepa, B., Pothan, L. A., & Thomas, S. (2011). Thermomechanical and spectroscopic characterization of natural fibre composites. *Interface Engineering of Natural Fibre Composites for Maximum Performance*, 241–274. https://doi.org/10.1533/9780857092281.2.241
Reddy, N., Han, S., Zhao, Y., & Yang, Y. (2013). Antimicrobial activity of cotton fabrics treated with curcumin. *Journal of Applied Polymer Science*, *127*(4), 2698–2702. https://doi.org/10.1002/APP.37613
Refaat, A. A. (2012). Biofuels from waste materials. In *Comprehensive Renewable Energy* (Vol. 5, pp. 217–261). Elsevier Ltd. https://doi.org/10.1016/B978-0-08-087872-0.00518-7
Rezaei, A., & Nasirpuri, A. (2018). Encapsulation of curcumin using electrospun almond gum nanofibers; fabrication and characterization. *International Journal of Food Properties*, *21*(1), 1608–1618.
Rosenau, T., Potthast, A., Sixta, H., & Kosma, P. (2001). The chemistry of side reactions and byproduct formation in the system NMMO/cellulose (Lyocell process). *Progress in Polymer Science*, *26*(9), 1763–1837. https://doi.org/10.1016/S0079-6700(01)00023-5
Rowell, R. M. (2005). Handbook of Wood Chemistry and Wood Composites. In *Taylor and Francis*. CRC Press. https://doi.org/10.1201/9780203492437
Royer, S. J., Wiggin, K., Kogler, M., & Deheyn, D. D. (2021). Degradation of synthetic and wood-based cellulose fabrics in the marine environment: Comparative assessment of field, aquarium, and bioreactor experiments. In *Science of The Total Environment* (Vol. 791). Elsevier.

https://doi.org/10.1016/J.SCITOTENV.2021.148060
Sachan, K., & Kapoor, V. P. (2007). Optimization of extraction and dyeing conditions for traditional turmeric dye. *Indian Journal of Traditional Knowledge*, *6*(2), 270–278.
Santos, P. S., Souza, L. K. M., Araujo, T. S. L., Medeiros, J. V. R., Nunes, S. C. C., Carvalho, R. A., Pais, A. C. C., Veiga, F. J. B., Nunes, L. C. C., & Figueiras, A. (2017). Methyl-β-cyclodextrin inclusion complex with β βcaryophyllene: Preparation, characterization, and improvement of pharmacological activitie. *ACS Omega*, *2*(12), 9080–9094. https://doi.org/10.1021/acsomega.7b01438
Sayyed, A. J., Deshmukh, N. A., & Pinjari, D. V. (2019). A critical review of manufacturing processes used in regenerated cellulosic fibres: viscose, cellulose acetate, cuprammonium, LiCl/DMAc, ionic liquids, and NMMO based lyocell. *Cellulose*, *26*(5), 2913–2940. https://doi.org/10.1007/S10570-019-02318-Y/FIGURES/14
Schradinger, F. (1905). Bacillus macerans, ein Aceton bildender Rottebacillus. Zentralblatt für Bakteriologie, Parasitenkunde, Infektionskrankheiten und Hygiene. *Abeteilung II*, *14*, 772–781.
Schweizer, E. (1857). *Das Kupferoxyd-Amrnoniak, ein Auflosungs-mittel fur die Pflanzenfaser*. https://scholar.archive.org/work/xd2obiom5jfnxahxrdrelegrhi/access/ia_file/crossref-pre-1909-scholarly-works/10.1002%252Fprac.18560690106.zip/10.1002%252Fprac.18570720115.pdf
Sharma, D., & Satapathy, B. K. (2021). Physicomechanical performance and encapsulation efficiency of β-cyclodextrin loaded functional electrospun mats based on aliphatic polyesters and their blends. *Journal of Biomaterials Science, Polymer Edition*, *32*(11), 1489–1513. https://doi.org/10.1080/09205063.2021.1925393
Sixta, H., Michud, A., Hauru, L., Asaadi, S., Ma, Y., King, A. W. T., Kilpeläinen, I., & Hummel, M. (2015). Ioncell-F: A high-strength regenerated cellulose fibre. *Nordic Pulp and Paper Research Journal*, *30*(1), 43–57. https://doi.org/10.3183/npprj-2015-30-01-p043-057
Sluiter, A., Hames, B., Ruiz, R., Scarlata, C., Sluiter, J., Templeton, D., & Crocker, D. (2011). *Determination of Structural Carbohydrates and Lignin in Biomass: Laboratory Analytical Procedure (LAP), NREL/TP-510-42618* (Vol. 2011, Issue April 2008).
Stanić, Z. (2017). Curcumin, a Compound from Natural Sources, a True Scientific Challenge – A Review. Plant Foods for Human Nutrition, 72(1), 1–12.
Stepan, A. M., Michud, A., Hellstén, S., Hummel, M., & Sixta, H. (2016). IONCELL-P&F: Pulp Fractionation and Fiber Spinning with Ionic Liquids. *Industrial and Engineering Chemistry Research*, *55*(29), 8225–8233. https://doi.org/10.1021/acs.iecr.6b00071
Sun, X. Z., Williams, G. R., Hou, X. X., & Zhu, L. M. (2013). Electrospun curcumin-loaded fibers with potential biomedical applications. *Carbohydrate Polymers*, *94*(1), 147–153. https://doi.org/10.1016/j.carbpol.2012.12.064
Sun, X. Z., Wu, J. Z., Wang, H. D., & Guan, C. (2021). Thermosensitive Cotton Textile Loaded with Cyclodextrin-complexed Curcumin as a Wound Dressing. *Fibers and Polymers*, *22*(9), 2475–2482. https://doi.org/10.1007/s12221-021-0334-1
Suzuki, S., Togo, A., Gan, H., Kimura, S., & Iwata, T. (2021). Air-Jet Wet-Spinning of Curdlan Using Ionic Liquid. *ACS Sustainable Chemistry and Engineering*, *9*(11), 4247–4255. https://doi.org/10.1021/acssuschemeng.1c00488

Swatloski, R. P., Spear, S. K., Holbrey, J. D., & Rogers, R. D. (2002). Dissolution of cellose with ionic liquids. *Journal of the American Chemical Society*, *124*(18), 4974–4975. https://doi.org/10.1021/ja025790m

Tsatsaroni, E., Liakopoulou-Kyriakides, M., & Eleftheriadis, I. (1998). Comparative study of dyeing properties of two yellow natural pigments Effect of enzymes and proteins. *Dyes and Pigments*, *37*(4), 307–315. https://doi.org/10.1016/S0143-7208(97)00069-7

Uekama, K., & Hirayama, F. (1978). Inclusion Complexation of Prostaglandin F2α with α-and β-Cyclodextrins in Aqueous Solution. *Chemical and Pharmaceutical Bulletin*, *26*(4), 1195–1200. https://doi.org/10.1248/CPB.26.1195

Viellers, A. (1891). *Sur la transformation de la fecule en dextrine par la ferment butyrique – ScienceOpen*. Compt. Rend. Acad. Sci. https://www.scienceopen.com/document?vid=535b2478-c9d1-40b0-a79e-f6f33ce6c8f3

Wang, H., Gurau, G., & Rogers, R. D. (2012). Ionic liquid processing of cellulose. *Chemical Society Reviews*, *41*(4), 1519–1537. https://doi.org/10.1039/c2cs15311d

Xiao, Z., Xu, W., Ma, J., Zhao, Y., Niu, Y., Kou, X., & Ke, Q. (2021). Double-encapsulated microcapsules for the adsorption to cotton fabrics. *Coatings*, *11*(4). https://doi.org/10.3390/coatings11040426

Yadav, V. R., Suresh, S., Devi, K., & Yadav, S. (2009). Effect of cyclodextrin complexation of curcumin on its solubility and antiangiogenic and anti-inflammatory activity in rat colitis model. *AAPS PharmSciTech*, *10*(3), 752–762. https://doi.org/10.1208/S12249-009-9264-8

Zhou, Y., & Tang, R. C. (2016). Modification of curcumin with a reactive UV absorber and its dyeing and functional properties for silk. *Dyes and Pigments*, *C*(134), 203–211. https://doi.org/10.1016/J.DYEPIG.2016.07.016

Zhu, C., Richardson, R. M., Potter, K. D., Koutsomitopoulou, A. F., Van Duijneveldt, J. S., Vincent, S. R., Wanasekara, N. D., Eichhorn, S. J., & Rahatekar, S. S. (2016). High modulus regenerated cellulose fibers spun from a low molecular weight microcrystalline cellulose solution. *ACS Sustainable Chemistry and Engineering*, *4*(9), 4545–4553. https://doi.org/10.1021/ACSSUSCHEMENG.6B00555/ASSET/IMAGES/LARGE/SC-2016-00555X_0010.JPEG